Reconstructed W(001) surface: distortion and phonons at $T=0$

A. Fasolino and E. Tosatti
International School for Advanced Studies, Strada Costiera 11, I-34100 Trieste, Italy
(Received 14 May 1986; revised manuscript received 10 November 1986)

Effective bulk and surface interatomic potentials are used to construct a quantitative description of the $c(2\times2)$ reconstruction of the *clean* W(001) surface. Appropriate Landau-Ginzburg Hamiltonians for the reconstruction are described, and numerical values for their parameters are obtained at $T=0$ from our effective Hamiltonian. The full phonon spectrum of the reconstructed surface is then calculated. Prominent surface modes and resonances characteristic of this reconstruction are identified and discussed in detail.

I. INTRODUCTION

The findings of Felter, Barker, and Estrup[1] and simultaneously by Debe and King[2] that the clean (100) surfaces of W and Mo undergo reconstruction have generated wide interest. A variety of studies have been carried out in order to clarify the nature of this phenomenon. Clearly the interest in these reconstructions has more than one facet. They are first of all interesting *per se,* as "intrinsic" surface phase transitions.[3] However, they are also important for the broader field of adsorbate ordering. It is becoming more and more evident in fact, that ordering phenomena on apparently inert surfaces also imply in many cases an accompanying reconstruction. It is important to understand the nature both of naturally reconstructed surfaces as well as "dormant" surfaces, which will reconstruct, once covered by some amount of adsorbate.

The main experimental facts concerning these reconstruction phenomena have been reviewed by Estrup *et al.*,[4] and also by King *et al.*[5,6] On the theoretical side, work has been done on several fronts, particularly in connection with (i) what is the microscopic origin of the reconstruction, and its energetics; (ii) what kind of statistical mechanics does one have at the reconstruction phase transition; (iii) how can one characterize the static distortion of the reconstructed surface lattice, and its vibrations about equilibrium.

We can briefly summarize the present status of these issues as follows:

(i) *Microscopic mechanism.* Following early suggestions that the reconstruction could be due to two-dimensional (2D) surface charge-density waves (CDW) of the half-filled surface states,[7,1] evidence has accumulated which indicates that the half-filled surface states indeed exist and are likely to be the driving force of these reconstructions.[8–16] On the other hand, it is now believed that the details of the reconstruction periodicity are almost certainly dictated by the underlying lattice, rather than by a 2D Fermi surface.[17] We have referred to this state of affairs as a "strong coupling CDW",[18] while others prefer to call it a "short-range Jahn-Teller effect."[19] The important issue, namely that the same surface would not reconstruct if its surface states were empty—as is actually the case for Ta(100) (Ref. 20) and Nb(100) (Ref. 21)—seems now well established. First-principle attacks on the energetics of the surface reconstruction which are beginning to appear[16] provide further support for this point of view.

(ii) *Statistical mechanics.* A Landau-Ginzburg theory of surface reconstruction phase transitions can be formulated based solely on symmetry. For W(100), one expects[7,18,22] the same universality class as an X-Y model with cubic anisotropy. Ying *et al.* have gone into considerable more detail, and have investigated the switching from pure X-Y (Kosterlitz-Thouless) to nonuniversal, roughly Ising-like behavior in the presence of cubic anisotropy.[23,24] Lau and Ying[25] also considered additional phase transitions induced by "renormalizing" the clean surface parameters with an "annealed" adsorbate, such as hydrogen. Related work has also been published by Yoshimori and co-workers.[26]

(iii) *Static distortion and phonons.* Prior to first-principle studies of surface reconstruction energetics, we have shown that the reconstruction problem can also be studied by a simplified lattice Hamiltonian.[27] Here, all electronic degrees of freedom are effectively integrated out and replaced by a phenomenological pairwise interaction between first surface neighbors only. Based on stability studies performed on slabs, this approach shows that the commensurate $c(2\times2)$ reconstruction of W(100), as well as the incommensurate reconstructions of Mo(100) may appear quite naturally, once these effective intrasurface forces are made sufficiently different from their bulk values. In particular, it is interesting that in this case incommensurability can arise due to strong competition between *direct* atom-atom forces in the surface and opposing *indirect* forces, that are mediated through the second and deeper layers.[28] Our effective-Hamiltonian approach and search for surface phonon instabilities has recently been adopted and modified by various authors.[26,29,30]

The purpose of this paper is to present the results of accurate and comprehensive calculations (based on the same effective lattice Hamiltonian as in Ref. 27, but with a new and better potential parametrization) of the detailed form of the reconstruction of W(100), of its energetics at $T=0$ including surface relaxation effects, and of the new surface phonon spectrum to be expected on the reconstructed surface. For special purposes, not involving either surface phonon spectra, incommensurate phases, or relaxation phenomena, two-dimensional simplified approaches as that of Hu and Ying[30] can be valuable. In the present

context, however, the use of a full three-dimensional approach is inescapable. In particular, the subtle phonon interactions leading to incommensurate instabilities occur via the second layer,[28] or even via coupling to the deep bulk [as in the so-called "incommensurate sandwich" mechanism].[31]

We start in Sec. II by introducing our lattice Hamiltonian based on different bulk and surface interatomic potentials. In this section we further discuss how a suitable phenomenological bulk pairwise potential may be chosen, particularly in connection with the helpful check provided by molecular dynamics. In Sec. III we introduce the parametrized surface potential, and discuss the general connection between instability of the unreconstructed surface and possible displacive reconstructions. In Sec. IV we determine the reconstruction parameters (static in-plane displacement of atoms in first, second, and deeper layers, as well as the change of relaxation of first layer relative to the second) which minimize the total energy. We compare in particular the energetics of different $c(2\times2)$ reconstructions, and discuss their relative stability at $T=0$. The total-energy differences can be approximately cast in the form of Landau-Ginzburg Hamiltonian, and this is done in general terms in Sec. V and more particularly for the $c(2\times2)$ reconstruction of W(001) with the inclusion of relaxation effects in Sec. VI. These Hamiltonians are of great usefulness for the purpose of acquiring a qualitative understanding of the mutual interplay of different order parameters. Also, when generalized to represent free energy differences, the Landau-Ginzburg Hamiltonians become crucial for the purpose of identifying universality classes for the reconstructed-to-disordered phase transitions.

The lattice vibrations of a clean reconstructed transition-metal surface have never so far been measured in detail. In Sec. VII we present the full surface phonon spectrum of the clean reconstructed W(100), calculated by our effective Hamiltonian. Important surface modes and resonances are identified, and pinpointed for possible future identification, e.g., by He or electron scattering experiments. Finally, a summary and a general discussion are given in Sec. VIII. In particular, we discuss qualitative expectations, based on mean-field theory reasoning, concerning finite temperature behavior, and possible surface phonon softening phenomena at the reconstruction phase transition.

II. EFFECTIVE LATTICE HAMILTONIAN FOR SURFACE RECONSTRUCTION

The occurrence of displacive reconstruction at low temperatures on the W(100) and Mo(100) surfaces obviously indicates that somehow a periodic surface lattice distortion acts to lower the total energy. Ideally, a reconstruction problem could then be studied by a total-energy formulation which should include both electronic and ionic degrees of freedom on a similar footing. The first relevant, if obvious, consideration is that the electronic densities and wave functions are changed drastically by the presence of a surface only within a finite and quite small depth, usually of the order of a few times K_F^{-1}.[32] The underlying semiinfinite bulk remains unaffected. Being intrinsically stable against lattice distortions, it will just basically resist elastically the onset of a displacive surface reconstruction.

The next question is, what happens in the first few atomic layers, which might favor a displacive reconstruction. Here the electronic structure is greatly disturbed with respect to the bulk, and the motivation must come from these perturbed electronic states. One qualitative, but very suggestive consideration that one can make about a bcc transition-metal surface is that such a surface must bear some similarities to a semiconductor surface. A semiconductor is covalently bonded in a bulk, and this implies a strong directional bond hybridization, and a gap. At a free clean semiconductor surface, though bonds are broken, rehybridization is not very strong, due to the presence of a gap (states whose energies are above the gap would have to be used in order to rehybridize). As a result, a semiconductor surface has half-filled "dangling bonds," and the necessity to saturate them provides a strong driving force for reconstructions, which are indeed observed.[33] The bulk bonding of a bcc transition metal can also be seen as partly "covalent" in a similar sense: the d density of states has two main "bonding" and "antibonding" peaks,[34] with a kind of pseudogap in between, where the Fermi level lies. The presence of a sharp density of states peak crossing E_F on clean bcc transition-metal surfaces is known (Refs. 35, 36, 7, 8, 9, and 10). The dangling bond nature of these states has been recently demonstrated by local density calculations,[11,12] which confirms the similarity to semiconductors.[37]

Similarly to early theories outlined for semiconductors,[33] the atoms of the outermost layers of W(100), and the electrons in its half-filled dangling bonds form a complicated coupled electron-lattice system. In order to make such a system tractable, one could in principle choose to integrate out the lattice degrees of freedom, and one would obtain an extra "excitonic-like" electron-hole attractive interaction,[33] leading to a gap or pseudogap in the electronic spectrum. The alternative possibility of integrating out the electronic degrees of freedom, resulting in an effective lattice problem, is in principle exactly equivalent. However, these two schemes may become quite different if they are handled by means of approximations, as invariably is the case. An effective lattice formulation is attractive, since once the electronic forces are modeled, the remaining lattice problem can be dealt with exactly. Then a number of detailed issues ranging from distortion geometries and energies, to lattice vibrations and all the way to statistical mechanics of the reconstruction phase transition, become immediately tractable.

In this spirit, we have used for the description of the W(100) clean surface, an effective (classical) lattice Hamiltonian where bulk atoms and surface atoms interact differently. That is,

$$H=T+V=\sum_l P_l^2/2M+\tfrac{1}{2}\sum_{\substack{l,m\\(\neq\langle l,m\rangle)}} V_B(\mathbf{R}_l-\mathbf{R}_m)+\tfrac{1}{2}\sum_{\substack{\langle l,m\rangle\\=\text{first surface neighbors}}} V_s(\mathbf{R}_l-\mathbf{R}_m)\,, \tag{1}$$

where the summations run over atoms ($\mathbf{R}_l$ denoting their coordinates) of a semiinfinite crystal, or equivalently of a n-layer slab. The bulk lattice properties of W are here supposed to be described by a two-body potential $V_B(R)$, to be suitably chosen.[38] The interaction of two surface atoms $V_s(R)$ is then in principle very different from that of two bulk atoms, due to the different surface electronic structure as discussed earlier. Strictly speaking, the interactions between a surface and a "bulk" atom (particularly a second-layer atom) should again be different from either V_B or V_s. It should be noted, however, that reconstruction and relaxation lead to a change of static interparticle distances near the surface, implying that also pairs connected by $V_B(R)$ interact in our model differently than in a bulk. Therefore, we will insist in our model Hamiltonian Eq. (1) that such interactions remain equal to $V_B(R)$. Moreover, we are not at present in a position to determine any of these interactions from first principles. Instead, we will phenomenologically parametrize both $V_B(R)$ and $V_s(R)$; and the introduction of yet more parametric freedom is neither desirable nor necessary. This will mean, that we in some way conventionally embody the whole spectrum of different atom-atom forces which occur near a surface into a unique interaction $V_s(R)$, vastly different from the bulk $V_B(R)$. We will furthermore take $V_s(R)$ to be short ranged. We have argued[17] that this should be appropriate for a strong-coupling situation, which is close to a short-range chemical bonding between surface atoms.

We write the general $V(R)$ (both bulk and surface) as a fourth-order power expansion, namely

$$V_i(R)=V_i^0+R_i^{0^2}\left[\alpha_i\left[\frac{R}{R_i^0}-1\right]+\frac{1}{2!}\beta_i\left[\frac{R}{R_i^0}-1\right]^2+\frac{1}{3!}\gamma_i\left[\frac{R}{R_i^0}-1\right]^3+\frac{1}{4!}\delta_i\left[\frac{R}{R_i^0}-1\right]^4\right] \tag{2}$$

where

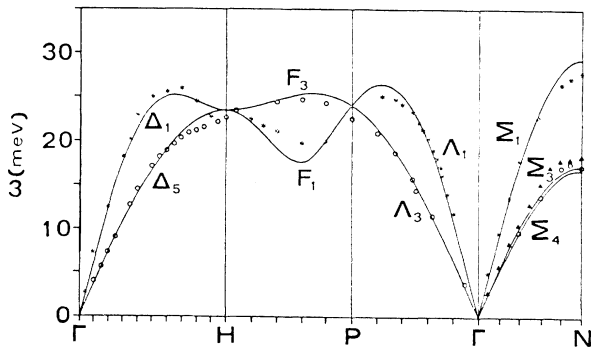

FIG. 1. Bulk phonon spectrum of tungsten as obtained by the phonon fitting of Ref. 39. Experimental points are taken from Brockhouse (Ref. 67).

$$\alpha_i=\left[\frac{1}{R}\frac{\partial V_i}{\partial R}\right]_{R=R_i^0},\quad \beta_i=\left[\frac{\partial^2 V_i}{\partial R^2}\right]_{R=R_i^0},$$
$$\gamma_i=\left[R\frac{\partial^3 V_i}{\partial R^3}\right]_{R=R_i^0},\quad \delta_i=\left[R^2\frac{\partial^4 V_i}{\partial R^4}\right]_{R=R_i^0}$$

represent harmonic and anharmonic force constants. In the bulk, we consider first-neighbor interactions ($i=1$) and second-neighbor interactions ($i=2$). There, R_i^0 is the equilibrium distance ($R_1^0=a_0\sqrt{3}/2$, $R_2^0=a_0=3.16$ Å for W). All further bulk interactions are taken to be zero. At the (001) surface ($i=s$) only first-neighbor intrasurface interactions are retained, with $R_s^0=a_0$. The bulk harmonic parameters satisfy $\alpha_1=-\alpha_2$ and are taken $\alpha_1=-0.03$ eV/Å^2, $\beta_1=4.60$ eV/Å^2, $\beta_2=3.29$ eV/Å^2 from the phonon fitting of Castiel *et al.*[39] In Fig. 1 we show the resulting bulk phonon spectrum of W.

The anharmonic parameters γ_1,γ_2 are determined by fitting the linear thermal expansion coefficient $\alpha=3.76\times10^{-6}$ K^{-1} and the linear temperature coefficient of the C_{44} elastic constant $\Lambda_{44}=-0.644\times10^{-4}$ K^{-1}.[40] Given an average potential energy per atom $U(a)$ for a local lattice parameter a, a crude but simple way to evaluate the thermal expansion coefficient α is the Einstein average

$$\langle a-a_0\rangle=\frac{\int_{-\infty}^{\infty}(a-a_0)\exp\{-[U(a)-U(a_0)]/k_BT\}da}{\int_{-\infty}^{\infty}\exp\{-[U(a)-U(a_0)]/k_BT\}da}\simeq a_0\alpha T\ .$$

Since $U(a)=\frac{1}{2}[8V_1(R=a\sqrt{3}/2)+6V_2(R=a)]$ we obtain, by inserting for V_1 and V_2 the form (2)

$$\frac{\alpha}{k_B}=-\frac{(\gamma_1+\gamma_2)}{6a_0^2(\beta_1+\beta_2)^2}\ . \tag{3}$$

In the quasiharmonic approximation the elastic constant change is obtained simply by recalculating C_{44} at $a=a_0(1+\alpha T)$,

$$\Lambda_{44}=\alpha\left[-1+\frac{\beta_2-\alpha_2+\gamma_1/3+2(\beta_1-\alpha_1)/3}{\alpha_2+(\beta_1+2\alpha_1)/3}\right] \tag{4}$$

giving $\gamma_1=-93.3$ eV/Å^2, $\gamma_2=-79.0$ eV/Å^2.

Since distortions at the surface are generally not small, we need to specify also bulk fourth-order anharmonicities δ_1,δ_2 as in Eq. (2). Though in principle we could try to determine δ_1,δ_2, e.g., from the quadratic temperature coefficients of thermal expansion and elastic constants, in practice it was found to be handier and safer to determine them by a simple molecular dynamics (MD) run of bulk W (which was performed with the help of C. Z. Wang), and with the bulk potential as specified by Eq. (2). As it turns out, the expansion curve is very dependent upon the choice of δ_1 and δ_2 already at relatively low temperatures.

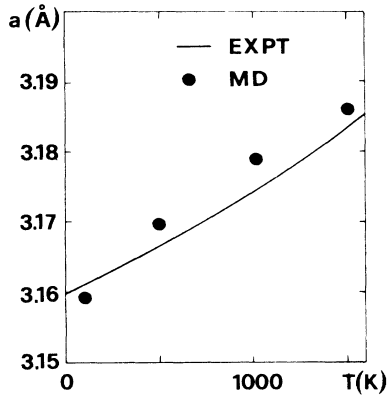

FIG. 2. Comparison of the experimental thermal expansion of bulk W with the molecular dynamics (MD) results obtained with the bulk potential described in Sec. II.

The best values yielding a reasonable low-temperature expansion as on Fig. 2 turned out to be $\delta_1=3.0\times10^3$ eV/Å^2, $\delta_2=1.5\times10^3$ eV/Å^2.[41] The constants V_i^0 determine very sensitively the crystal structure in the MD calculation. A stable bcc structure with the correct cohesive energy of $E_c=8.66$ eV/atom was obtained with $V_1^0=-1.25$ eV, $V_2^0=-1.21$ eV.

Clearly no such fitting is possible for the four surface parameters $\alpha_s,\beta_s,\gamma_s,\delta_s$. They therefore remain free adjustable parameters of this theory. In the following chapter, we will show that the *harmonic* surface force constants (SFC) α_s,β_s closely determine either the stability of the ideal (unreconstructed) surface, or the type of reconstruction of the surface. In the subsequent Sec. IV, on the other hand, the *anharmonic* SFC γ_s and δ_s will be shown to determine the magnitudes of the $T=0$ reconstruction distortions, and other important features.

III. HARMONIC STABILITY AND INSTABILITIES OF THE IDEAL (UNRECONSTRUCTED) SURFACE

As discussed above our bulk potential yields a stable bcc bulk crystal. We want now to determine the stable surface structure of a semiinfinite crystal whose first-layer atoms interact via a given surface potential $V_s(R)$. Clearly, reconstruction will occur if a rearrangement with different periodicity from the ideal can yield lower energy.

In principle, the unreconstructed surface could be, as a function of $\alpha_s,\beta_s,\gamma_s,\delta_s$, either (a) a stable energy minimum (no reconstruction), (b) a metastable energy minimum, i.e., not the lowest minimum, or (c) an unstable extremum, such as a maximum or a saddle point.

Our goal is to uncover and pinpoint regions of SFC values where either of these possibilities is realized. It is, in fact, generally difficult to discover "first-order" reconstructions, of type (b), without some kind of random sampling of the configuration space. We have not pursued this possibility further, as it did not appear a likely one. Fresh MD results that are currently being examined confirm this guess.[42] Surface lattice instabilities of type (c) can be found by a standard linear stability analysis. In practical terms, this amounts to asking whether there are in the ideal surface any unstable phonon modes, i.e., negative values for some $\omega^2_{\mathbf{q},\lambda}$ ($\mathbf{q},\lambda$ denoting, respectively, wave vector and branch).

Given a surface phonon branch which has negative ω^2, the implication is that the time evolution of such a state will change from oscillatory to exponentially growing $e^{\omega t}$. The growth will eventually be stopped by anharmonicity, and the final stable configuration is generally close to the one obtained by "freezing in" the fastest growing mode eigenvector, which is the lowest, over the initially ideal surface.

Slab calculations are a particularly simple way to study the surface stability and surface phonons.[43] We here give details following closely our earlier work.[27] We take an n-layer slab (usually $n=25$ is quite sufficient, though, occasionally we have used up to $n=75$) and solve the eigenvalue problem

$$[\underline{D}(\mathbf{q})-M\omega^2_{\mathbf{q},\lambda}\underline{I}]\mathbf{u}_\lambda(\mathbf{q})=0\ , \tag{5}$$

where $\mathbf{q}$ is the 2D wave vector and $\underline{D}(\mathbf{q})$ is the dynamical matrix. For a central potential, that can be written explicitly as

$$D^{ll'}_{\mu\nu}(\mathbf{q})=\sum_{l'',\mathbf{r}_i(l'')}\left[\alpha_i\delta_{\mu\nu}+(\beta_i-\alpha_i)\frac{R''_{i\mu}R''_{i\nu}}{|R^0_i|^2}\right]\times(\delta_{ll'}-e^{i\mathbf{q}\cdot\mathbf{r}_i(l'')}\delta_{l'l''})\ , \tag{6}$$

where $\mathbf{R}_i=\mathbf{r}_i+(la_0/2)\hat{\mathbf{z}}$ is the coordinate of an atom on layer l [$\mathbf{r}_i$ being the (x,y) projection of $\mathbf{R}_i$], $\mu\nu$ are Cartesian coordinates, and α_i,β_i take the value $\alpha_1,\beta_1,\alpha_2,\beta_2,\alpha_s,\beta_s$ for first, second, and intrasurface neighbors, respectively.

As a function of the harmonic SFC α_s and β_s, we obtain the stability diagram of Fig. 3. Each region in this diagram signifies either stability of the ideal surface or an instability of some type. For $\alpha_s=\alpha_2$, $\beta_s=\beta_2$ the ideal surface is stable, and the surface phonons of Castiel *et al.*[39] are reproduced. Surface stability is only lost for very large changes of surface force constants. Within the present scheme instabilities occur at the Brillouin zone (BZ) points L and M (see inset in Fig. 3) and in their neighborhood. An analysis of the details of each instability and possible reconstruction implied by this phase diagram is given in Appendix A.

The regions I_1 and I_2 are incommensurate, i.e., $\omega^2_{\mathbf{q},\lambda}$ is minimal for values of $\mathbf{q}$ such that $\mathbf{q}\cdot\mathbf{R}\neq2\pi n$, where $\mathbf{R}$ is some direct lattice vector and n is a small integer. It may be at first sight surprising to find incommensurate instabilities in a system with short-range forces. What happens is that the direct surface interaction V_s and the bulk-mediated forces compete in determining the actual surface arrangements. It is known from many other examples that incommensurability is a very common way to resolve this competition. We believe this aspect to be of importance for the incommensurate reconstructions of Mo(001) (Ref. 28) and of W(001):H (Ref. 17). However, since our focus is on the $c(2\times2)$ commensurate W(001) a

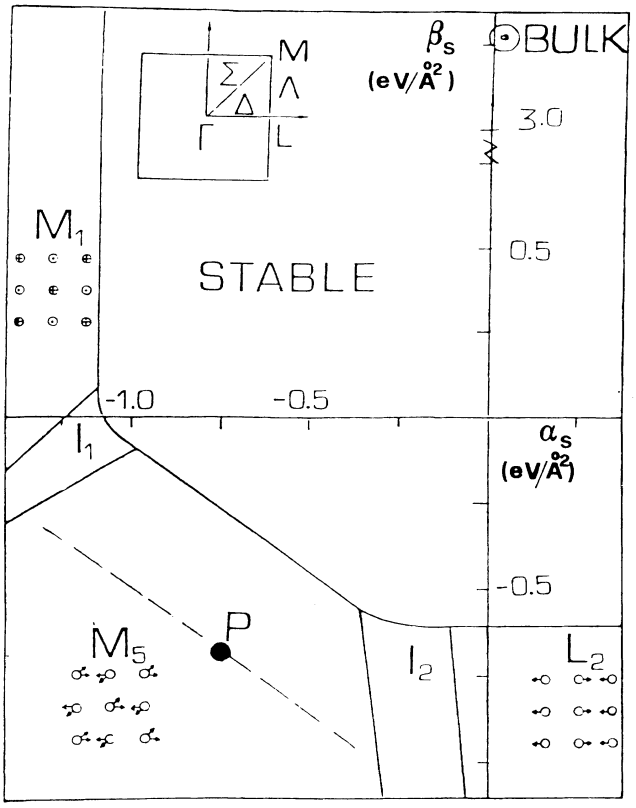

FIG. 3. Stability diagram of the ideal W(001) surface as a function of the harmonic SFC, α_s,β_s (in units of eV/Å^2). A sketch of the eigenvector of the soft mode on the first layer is shown for the three regions corresponding to commensurate reconstructions. Two types of $c(2\times2)$ distortions are indicated in the M_5 region, namely $\langle 11\rangle$ and $\langle 10\rangle$ (they are degenerate within the harmonic approximation, and acquire a different energy only with the inclusion of anharmonic forces). In the inset the Brillouin zone (BZ) of a bcc (001) surface. All calculations in this paper are performed for the point P, as representative of clean W(001) at $T=0$. Other points on the dashed line inside the M_5 region would approximately yield the same distortion magnitude and energy gain.

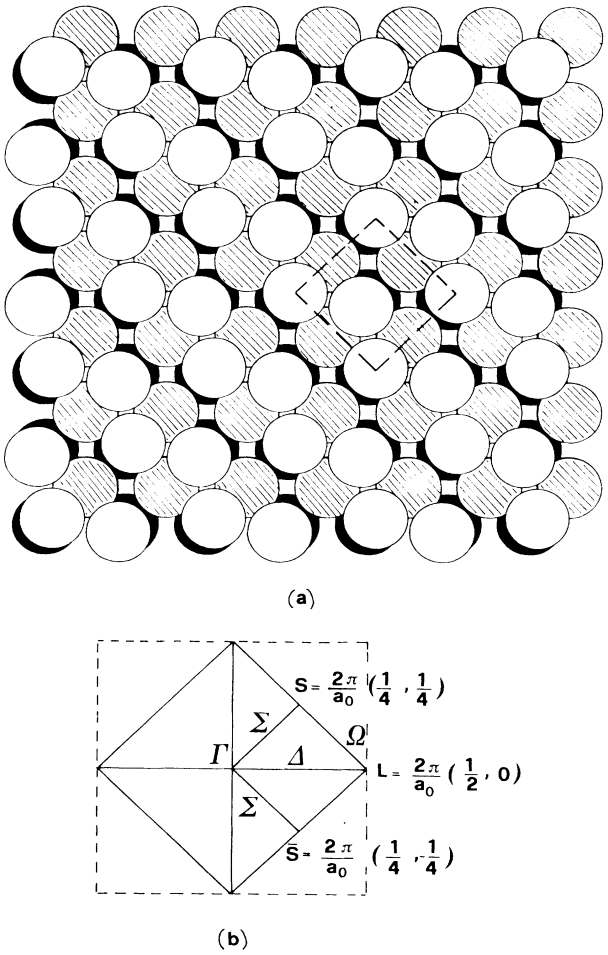

FIG. 4. (a) Sketch of atomic positions on the W(001)$c(2\times2)\langle 11\rangle$ reconstructed surface. For clarity the M_5 distortion magnitude in this figure is approximately 1.5 times bigger than the true distortion ρ_0 (in this work, $\rho_0\sim0.22$ Å). Second layer atoms are shaded, third layer atoms are black. (b) BZ of the reconstructed surface inscribed in the BZ of the ideal surface (dashed).

detailed discussion of the nature of the incommensurate phases I_1 and I_2 is postponed until Appendix B.

The $c(2\times2)$ reconstruction obtained by freezing in a twofold degenerate M_5 surface phonon mode has all the characteristics expected for a description of the $c(2\times2)$ state of clean W(001).[7,27] They are the following.

(i) Correct periodicity, leading to a $c(2\times2)$ unit cell.

(ii) The M_5 eigenvector is mostly confined in the first layer, and for a particular choice of phase, is very similar to the Debe-King model of reconstruction, found by low-energy electron diffraction (LEED) (Ref. 2) and shown in Fig. 4.

(iii) Surface symmetry is reduced for an $M_5\langle 11\rangle$ distortion from C_{4v} to C_{2v}, which agrees with LEED observations.

(iv) Double degeneracy of M_5 implying two types of domains that can be selectively enhanced in presence of, e.g., oriented steps, as observed.[4,5]

(v) The switching from $c(2\times2)\langle 11\rangle$ to $c(2\times2)\langle 10\rangle$ reconstruction upon H adsorption can be readily understood as a switch from an $M_5\langle 11\rangle$ to another $M_5\langle 10\rangle$ distortion, which differ only by small anharmonic terms.

In detail, the suggested M_5 distortion at and below the surface can be written as

$$\mathbf{R}_{il}-R^0_{il}=\rho_0\mathbf{u}^{M_5}_{il}=\rho_0\epsilon_{M_5}(l)(\hat{x}+\hat{y})\times\left[\exp\left[i\frac{2\pi}{a_0}(\tfrac{1}{2},\tfrac{1}{2})R^0_{il}\right]+\text{c.c.}\right], \quad (7)$$

where the normalized eigenvector $\epsilon_{M_5}(l)$ decays exponentially with the layer number l,[44] as shown in Fig. 5, and ρ_0

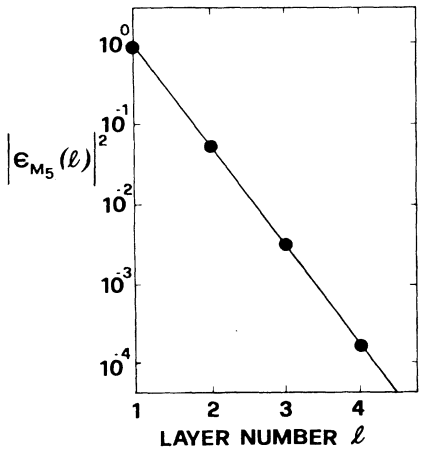

FIG. 5. Square distortion amplitude for the M_5 soft mode as a function of the depth. The topmost surface layer corresponds to $l=1$. We expect the $c(2\times2)$ distortion magnitude to decay in this way below the first layer.

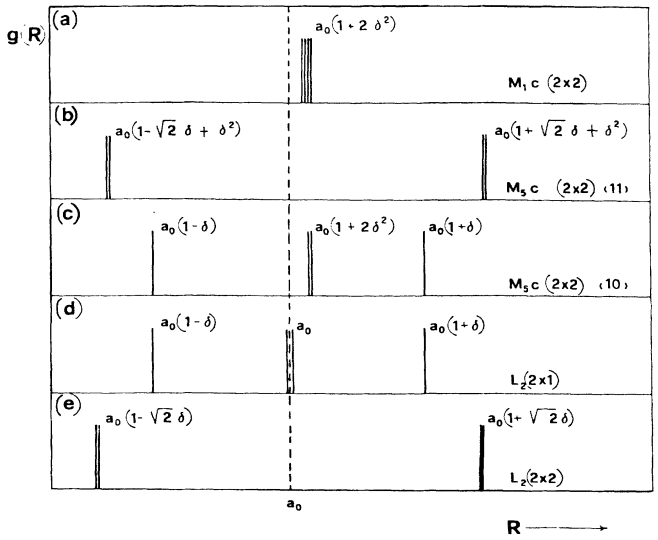

FIG. 6. Schematic $T=0$ surface pair distribution function for the M_1, M_5, and L_2 reconstructions. In cases a,b,c, the center of the distribution is at $a>a_0$, while for cases d,e it is exactly at a_0. Hence, a,b,c, are preferred for forces that are repulsive within the surface.

is an overall amplitude, which plays the role of order parameter, as discussed in detail later.

Before we move on to examine more closely the energetics of the lattice distortion, we wish to make a few general comments about the connection between the surface forces and the type of reconstruction.

All in-plane reconstructions seem to require the harmonic second-order SFC β_s to be opposite in sign and about $\frac{1}{4}$ the bulk magnitude. Incidentally, this finding bears an interesting qualitative analogy with that by Binder and Landau,[45] who noted that an antiferromagnetic surface reconstruction on a bulk Ising ferromagnet will also occur when $J^{\rm surf}=-J^{\rm bulk}/4$.

The $L_2(2\times1)$ or (2×2) reconstruction which consists of forming pairs or quartets of surface atoms is formed when the surface interaction is attractive ($\alpha_s>0$). The M_5 and M_1 $c(2\times2)$ states on the other hand, are preferred when the surface forces are repulsive ($\alpha_s<0$). There is a very simple way to argue about which reconstructions will be favored by an attractive or repulsive interaction. As indicated in Fig. 6, with a repulsive V_s, the pair distribution function obviously favors the three possible $c(2\times2)$'s (M_5 and M_1) over either (2×2) or (2×1) (L_2) as indeed found in our phase diagram of Fig. 3.

Returning to W(001), the presence of $c(2\times2)$ reconstructions indicates a repulsion between surface atoms.[46] It is not simple to trace the reason why two surface atoms on W(001) effectively repel, back to a straightforward physical, or chemical reasoning. However, it is important to keep in mind that V_s is only an effective interaction, which can embody more than one mechanism. For example, it would be entirely plausible to suppose that in reality, due to the surface contraction—which is omnipresent on clean metal surfaces—the indirect force via the second layer could in fact become repulsive, due to core-core overlap. Our effective Hamiltonian Eq. (1), though making no explicit provision for surface contraction, is able nevertheless to handle a situation of this kind as well.[47]

IV. ENERGETICS AND PARAMETERS OF RECONSTRUCTION

Once α_s and β_s take up values outside of the stability region, the ideal surface no longer minimizes the effective lattice potential energy of Eq. (2). The ensuing distortion, if it is not too large, is expected to be close in form to the fastest growing mode eigenvector of Eq. (7). The anharmonic forces—both bulk and surface—act to limit the growth of the distortion. In particular, a crucial role should be played, like in other structural phase transitions, by steric hindrance of hard atomic cores.

Our task at this point consists of the following.

Comparing the energetics of different types of distortion, and choose the most convenient, at $T=0$. In doing so, additional surface displacements, compatible with the known facts and with symmetry (e.g., relaxation of the first-second layer distance), must be allowed for.

Choosing a set of values $\alpha_s,\beta_s,\gamma_s,\delta_s$ which within our phenomenological scheme can represent as closely as possible the experimental situation for W(001).

Extracting any new information that this simple $T=0$ model may provide. Such are, for example, the energetic gain upon distortion, the change of surface relaxation, etc.

Given a starting set of SFC $\alpha_s,\beta_s,\gamma_s,\delta_s$ we calculate the energy change as

$$\Delta E_\lambda(\rho_\lambda,h)=V\{\mathbf{R}_{il}+\rho_\lambda\mathbf{u}_{il}^\lambda+h\hat{z}\delta_{l,0}\}-V\{\mathbf{R}_{il}^0\}\ , \qquad (8)$$

where $V\{\mathbf{R}_{il}\}$ is the effective lattice potential-energy functional of Eq. (1), λ denotes the symmetry and type of distortion (i.e., $M_5\langle11\rangle$, or $M_5\langle10\rangle, M_1,\ldots$), $\mathbf{u}_{il}^\lambda$ is the corresponding fastest growing normalized eigenvector, as given for example by Eq. (7), ρ_λ is the reconstruction or-

der parameter amplitude already introduced in Eq. (7), and h is a first-second layer relaxation with respect to the equilibrium value of the unreconstructed surface. Our bulk parametrization yields for the unreconstructed surface an initial slight outwards relaxation of 0.01 Å. This is, of course, at variance with an experimentally known slight contraction of about same magnitude.[48] In fact, we have used a simple two-body potential to describe bulk tungsten, and such potential cannot yield a surface contraction. This notwithstanding, we have all reasons to believe, that the change of relaxation with reconstruction is still very reasonable in our scheme. In fact, we will find that such relaxation changes do make a nonnegligible contribution in qualitative agreement with the recent results of Ref. 16.

We are primarily interested in describing the $c(2\times2)\langle 11\rangle$ (in-plane) reconstruction, which is found experimentally. Therefore α_s and β_s must lie inside the M_5 region in the $T=0$ phase diagram of Fig. 3. However, the $c(2\times2)\langle 11\rangle$ and the $c(2\times2)\langle 10\rangle$ reconstruction are energetically degenerate, so long as the system is purely harmonic. A difference between the two arises due to the presence of anharmonicities (both bulk and surface). Hence, it is not surprising to find that a sharp divide exists in a (γ_s,δ_s) parameter plane, between a region where the $\langle 11\rangle$ distortion prevails, and another where the $\langle 10\rangle$ prevails. This does indeed happen, as exemplified by Fig. 7 for a particular, but reasonable choice of α_s,β_s. Choosing a point on either sides of this divide leads to total-energy curves, as a function of distortion amplitude ρ_0 and of relaxation change h_0, such as those shown in Fig. 8.

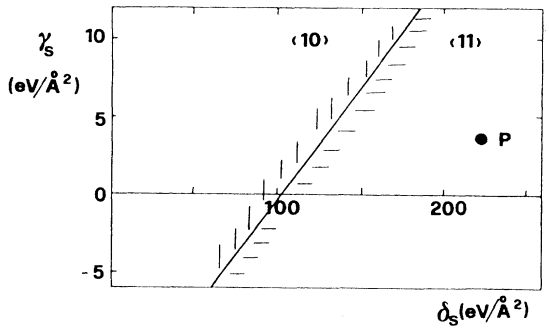

FIG. 7. Stability diagram as a function of the anharmonic SFC γ_s,δ_s for α_s,β_s fixed at the value of the point P. On the right-hand side of the oblique line, the energy of the $c(2\times2)\langle 11\rangle$ is lower than that of the $c(2\times2)\langle 10\rangle$ and vice-versa.

We see that (i) the anharmonic forces block the reconstruction magnitude, as expected, and (ii) the surface acquires an extra outward relaxation, upon reconstruction, corresponding to an extra energy gain of about 15%. This relaxation is bigger for the $\langle 11\rangle$ distortion, than for the $\langle 10\rangle$ distortion. This can be understood in simple terms by noting that for a $\langle 11\rangle$ distortion the first-layer atoms have to climb directly over the second layer repulsive cores, while this does not happen for a $\langle 10\rangle$ distortion. At present, it is difficult to select, as stated, a surface potential (or "point" P in our parameter space) P

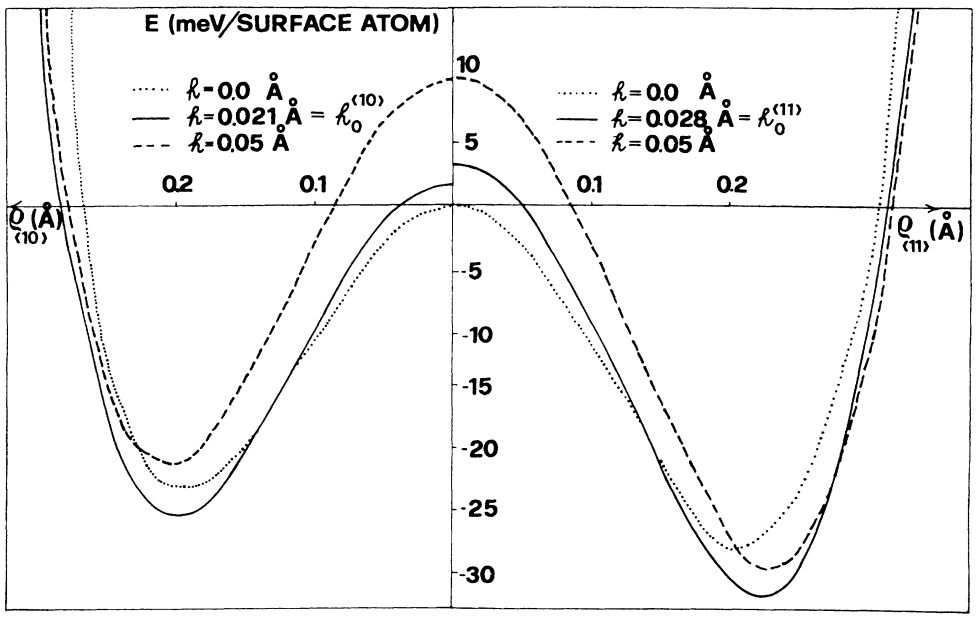

FIG. 8. Distortion energy as a function of the $c(2\times2)$ distortion magnitude along 11 and 10. The full line is calculated with the potential parameters as in Table I, for the equilibrium value of the relaxation $h=h_0$. The dotted line for $h=0$ which minimizes the energy of the ideal surface. The dashed line for $h>h_0$ is also included, showing that h_0 is optimal.

$=(\alpha_s,\beta_s,\gamma_s,\delta_s)$ as representative of the clean W(001) surface.

Our best guess is based on the following.

(1) The harmonic forces α_s,β_s must be such that the M_1 (vertical) instability does not occur, but is also not too far from occurring. We argue that this should be the case, because of the similarity of W(001) to Mo(001). We believe in fact that Mo(001) falls inside the incommensurate area I_1 of Fig. 3.[27,28] This region I_1 represents the borderline between M_5 and M_1 instability. Moreover, we believe[28] that the apparent discrepancy between LEED and field-ion microscopy (FIM) studies of W(001) could be understood as due to a field-induced switching from M_5 to M_1 reconstruction,[49] and this is more likely to happen if P is close to the M_1 region.

(2) The anharmonic forces γ_s,δ_s must be such that the $c(2\times2)\langle 11\rangle$ is only marginally stable over the $c(2\times2)\langle 10\rangle$ reconstruction. Our argument is based on the fact that a very small amount of annealed hydrogen, between 0.11 and 0.16 monolayers, is able to cause the switch from $\langle 11\rangle$ to $\langle 10\rangle$.[4,50,51]

(3) The distortion magnitude ρ_0, which depends very strongly upon both (α_s,β_s) and (γ_s,δ_s), should be not very far away from the well-established order of magnitude of about 0.2 Å (measured at low temperatures).[4,5]

(4) The static coherence length $\xi=2\pi/\delta q$ related to the wavevector δq of the critical **k**-space region, should be in the range of experimental values, i.e., $\xi=10$–15 Å.[52,4,5,27]

(5) All phonons of the reconstructed surface must be stable at $T=0$.

Our best choice of potential parameters, and resulting calculated quantities is given in Table I. There is a large amount of arbitrariness in this choice, which could be further reduced, given more experimental input. The available freedom in the choice of α_s,β_s is visualized by the dashed line, inside the M_5 region of Fig. 3. Pairs of α_s,β_s lying on that line (for fixed γ_s,δ_s) basically all yield reasonable distortion features. For α_s more negative, however, the system becomes prone to vertical (M_1) distortions, a tendency which disappears as α_s increases. Recent *ab initio* total-energy calculations provide a picture qualitatively similar to ours.[16] However we find that a larger energy gain of about 30 meV fits better than their value of about 10. A preliminary MD study of this surface with the present potential indicates indeed a $c(2\times2)$ reconstruction and a phase transition around room temperature.[42] Other interesting simplified electronic structure approaches which have recently appeared yield either no reconstruction for clean W(001) (Refs. 15 and 53)—contrary to experiment—or a reconstruction with an energy gain again lower than 10 meV/surface atom,[54] which we believe to be much too small.

V. LANDAU-GINZBURG HAMILTONIANS

In this section we wish to establish connection between the energy changes calculated in the previous section and the phenomenological approach of Landau-Ginzburg Hamiltonians (LGH). In that approach the change of energy (or free energy at $T=0$) upon reconstruction is cast in the form of a power series of one or more order parameters, plus gradient terms to account for inhomogeneous situations. While the nature of the order parameter is dictated by physical considerations, the detailed form of the expansion relies solely on symmetry [see, e.g., (55)].

A LGH is useful in several respects. Firstly, it provides a very simple and compact picture of one or more competing distortions, as controlled by very few parameters. This is in contrast with the detailed microscopic picture that is usually quite involved. Secondly, it explains universality, since in that approach entirely different physical situations may be described by formally identical Hamiltonians. Thirdly, it is valid at all temperatures, and thus it shows how phase transitions occur when one or more parameters are made temperature dependent.

We will present here several types of LGH. First, we discuss the simplest Hamiltonians applicable to each reconstruction that appears on the stability diagram of Fig. 3. These are the following: (1) M_5, (2) M_1, (3) L_2, and (4) I_1 or I_2 (incommensurate). Subsequently, in Sec. VI, we will focus on the specific point $P=(\alpha_s=-0.75$ eV/Å^2, $\beta_s=-0.94$ eV/Å^2, $\gamma_s=3.76$ eV/Å^2, $\delta_s=225.67$ eV/Å$^2)$ which we take to describe the $c(2\times2)\langle 11\rangle$ distortion of the clean W(001) surface, and work out all details, including numerical values of the parameters in the LGH, the effect of the relaxation, and the relationship to the surface phonon spectrum.

(1) *M_5 plane distortion (twofold degenerate).* Here we need a two-dimensional order parameter$=\rho e^{i\varphi}=(u,\bar{u})$ where u is the distortion magnitude along $\langle 10\rangle$ and $\bar{u}$ that along $\langle 01\rangle$:

TABLE I. Numerical values for parameters describing W-W interactions [first and second bulk neighbors, and (001) surface neighbors], and of calculated distortion magnitude, relaxation change, energy gain, surface vibration frequencies, and phase coherence length of the reconstructed W(001) surface.

α_1 (eV/Å^2)	−0.03	α_2 (eV/Å^2)	0.03	α_s (eV/Å^2)	−0.75
β_1 (eV/Å^2)	4.60	β_2 (eV/Å^2)	3.29	β_s (eV/Å^2)	−0.94
γ_1 (eV/Å^2)	−93.3	γ_2 (eV/Å^2)	−79.0	γ_s (eV/Å^2)	3.76
δ_1 (eV/Å^2)	3.0×10^3	δ_2 (eV/Å^2)	1.5×10^3	δ_s (eV/Å^2)	−0.75
ρ_0 (Å)	0.225	h_0 (Å)	0.028	ΔE (meV/surf. atom)	−31.2
ω_T (meV)	4.7	ω_Z (meV)	9.2	ω_L (meV)	10.3
ω_{L_2} (meV)	28.9	ω_{L_1} (meV)	32.1	$d\omega_T^2/d\rho$ (meV^2/Å)	−1.43
ξ_{phase}[a] (Å)	12				

[a]Approximate value along the (11) direction (see Sec. VI).

$$\Delta E_{M_5}=\int d^2x\{-r(u^2+\bar{u}^2)+a(u^2+\bar{u}^2)^2+bu^2\bar{u}^2 +J_0[(\nabla u)^2+(\nabla\bar{u})^2]\}$$
$$=\int d^2x\{-r\rho^2+a\rho^4+b\rho^4\sin^2(2\varphi)/4 +J_0[(\nabla\varphi)^2+\rho^2(\nabla\varphi)^2]\}\ , \quad (9)$$

where r,a,J_0 are positive at $T=0$,[7] and the expansion is limited to the fourth order in the order parameters and to the second order in the gradients.

It is clear from this Hamiltonian that a homogeneous distortion will be $c(2\times2)\langle 11\rangle$ if $b<0$ (that is, it is then convenient to have $\langle\varphi\rangle=\pi/4$, $3\pi/4$, etc.), and $c(2\times2)\langle 10\rangle$ if $b>0$ (when $\langle\varphi\rangle=0$, $\pi/2$, etc., prevails). The switching from $\langle 11\rangle$ to $\langle 10\rangle$ is supposed to take place experimentally with adsorption of hydrogen (Refs. 4, 50, 51, 25, and 17). These two situations in fact correspond to the microscopic energy balance of Fig. 8.

From the phase transition point of view, this Hamiltonian represents an X-Y model with cubic anisotropy, whose critical behavior is expected to be interesting and nonuniversal. These aspects have been discussed by various people.[56,22,23]

(2) *M_1 vertical distortion (nondegenerate).* By calling v the nondegenerate order parameter, we have simply

$$\Delta E_{M_1}=\int d^2x[-Rv^2+Av^4+J_1(\nabla v)^2]\ . \quad (10)$$

This Hamiltonian gives rise to a phase transition that falls in the same universality class as the 2D Ising model.[57]

(3) *L_2 planar distortion (two degenerate inequivalent k points).* The two-dimensional order parameter can be again written as $\rho e^{i\varphi}=(w,\bar{w})$, where w is the amplitude of an L_2 distortion at

$$\mathbf{q}=(1/2,0)2\pi/a_0=(1,0)$$

and $\bar{w}$=that of an L_2 distortion at

$$\mathbf{q}=(0,1/2)2\pi/a_0=(0,1)\ .$$

This LGH is identical in form to Eq. (9) for an M_5 distortion and similar considerations are applicable. In this case a (2×1) reconstruction occurs for $b>0$, while a (2×2) unit cell is formed for $b<0$.

(4) Incommensurate distortions I_1. As detailed in Appendix B, the incommensurate phases arise because of the competition between tendencies to distort at the same time vertically and horizontally. Hence, we must include both types of degrees of freedom, which leads to a three component order parameter $=(u,\bar{u},v)=(\rho,\vartheta,\varphi)$. The Hamiltonian is the following:

$$\Delta E_{I_1}=\int d^2x\left\{-r(u^2+\bar{u}^2+v^2)+a(u^2+\bar{u}^2+v^2)^2 +\Delta v^2+Av^4+bu^2\bar{u}^2+b_1(u^2+\bar{u}^2)v^2 -\delta\left[\left(u\frac{\partial v}{\partial x}-v\frac{\partial u}{\partial x}\right)+\left(\bar{u}\frac{\partial v}{\partial y}-v\frac{\partial\bar{u}}{\partial y}\right)\right] +J_0[(\nabla u)^2+(\nabla\bar{u})^2]+J_1(\nabla v)^2\right\}\ . \quad (11)$$

Here the term Δv^2 accounts for the energy splitting between M_5 and M_1 modes (see Appendix B, Fig. 16). In this respect the present problem is somewhat similar to that of a ferroelectric in an external field[58,59] (proportional to Δ). The incommensurability is driven by the "Lifshitz" term proportional to δ. The competition leading to incommensurability occurs between u and v in the x direction, and between $\bar{u}$ and v in the y direction. Hence, in both cases, the coupling of the horizontal to the vertical displacement drives the incommensurability.

It is interesting at this point to make contact between the specific LGH [Eq. (11)] and the general symmetry-based LGH form (as given, e.g., by Mukamel and Krinsky[57]). Following that general formulation, a two-dimensional incommensurate distortion of an originally C_{4v} undistorted system is described by two complex order parameters ψ_1 and ψ_2. The incommensurate order parameters consists in this case of a star of four inequivalent k points (q_0,q_0), $(-q_0,-q_0)$, $(-q_0,q_0)$, $(q_0,-q_0)$. For example, we can take ψ_1,ψ_1^* to be the (complex conjugate) amplitudes of the first two k points, and ψ_2,ψ_2^* those of the latter two. Using the standard rules of constructing C_{4v} invariants up to the fourth order plus gradient terms up to second order, we get

$$\Delta E_{I_1}=\int d^2x\{-r(|\psi_1|^2+|\psi_2|^2)+\bar{a}(|\psi_1|^2+|\psi_2|^2)^2 +\bar{b}|\psi_1\psi_2|^2+\bar{J}(|\nabla\psi_1|^2+|\nabla\psi_2|^2)\}\ . \quad (12)$$

At first sight, the general LGH [Eq. (12)] looks quite different from our previous expression Eq. (11). However, the two expressions become identical, once we recognize that the incommensurate order parameters ψ_1,ψ_2 can be approximately constructed in terms of amplitudes u, $\bar{u}$, and v at the nearby commensurate k point M. They are simply given by

$$\psi_1=\exp(i\,\delta\mathbf{q}\cdot\mathbf{r})(u+i\eta v)\ ,$$
$$\psi_2=\exp(i\,\delta\mathbf{q}\cdot\mathbf{r})(\bar{u}+i\eta v)\ , \quad (13)$$

where $\delta\mathbf{q}$ is the distance to the near commensurate point, and η is a numerical coefficient. By substituting Eq. (13) into Eq. (12), we recover Eq. (11) by neglecting terms of order $(\delta q)^2$ or higher, and by identifying parameters as follows:

$$r=\bar{r},\quad a=\bar{a}\ ,$$
$$A=\bar{a}(2\eta^2-1)^2+2\bar{a}(2\eta^2-1)+\bar{b}\eta^4\ ,$$
$$\Delta=-\bar{r}(2\eta^2-1),\quad b=\bar{b}\ ,$$
$$b_1=\bar{b}\eta^2+2\bar{a}(2\eta^2-1)$$
$$\delta=\bar{J}2\eta\,|\,\delta\mathbf{q}\,|\ ,\ J_0=\bar{J},\ \text{and}\ J_1=2\eta^2\bar{J}\ .$$

Summing up, the physical fact that both in plane displacements u and $\bar{u}$ couple to the same vertical displacement v reduces the order parameter dimensionality from its general value of 4, as in Eq. (12), down to three, as in Eq. (11).

The complete form [Eq. (11)] of the LGH for the I_1 incommensurate phase has not to our knowledge been given before. It simplifies to a two-component problem, analogous to the ferroelectric in an external field of Refs. 58

and 59, once one of the two components u or $\bar{u}$ is set equal to zero. In this case the problem implies the existence of discommensurations [or "soliton lattice" (Ref. 60)] between regions where the order parameter is predominantly u (or $\bar{u}$) and narrower regions where the order parameter is close to v. A statistical mechanical study of this situation has been given by Ying.[61]

In general, however, the simultaneous presence of a third ("Heisenberg-like") component of the order parameter is not *a priori* negligible. The full problem appears actually much more complicated. It may be useful to transform this Hamiltonian from the form of Eq. (11) into polar coordinates, by putting

$$(u,\bar{u},v)=(\rho\sin\vartheta\cos\varphi,\rho\sin\vartheta\sin\varphi,\rho\cos\vartheta)$$

whence

$$\begin{aligned}\Delta E_{I_1}=\int d^2x\{&-r\rho^2+a\rho^4+\rho^4[b\sin^2 2\varphi(2\sin^2\vartheta-\sin^2 2\vartheta)+2b_1\sin^2 2\vartheta]+\Delta\rho^2\cos^2\vartheta+A\rho^4\cos^4\vartheta\\&+\delta\rho^2[\vartheta'_x\cos\varphi+\vartheta'_y\sin\varphi+\sin 2\vartheta(\varphi'_y\cos\varphi-\varphi'_x\sin\varphi)/2]\\&+J_0\rho^2[(\nabla\vartheta)^2\cos^2\vartheta+(\nabla\varphi)^2\sin^2\vartheta]+J_1\rho^2(\nabla\vartheta)^2\sin^2\vartheta\}\ ,\end{aligned}\tag{14}$$

where an additional ("phase-only") approximation of constant amplitude, $\nabla\rho=0$, has been introduced.

Equation (14) represents a functional $\Delta E=\Delta E[\vartheta(r),\varphi(r)]$ of two phases ϑ,φ. The minimization of this functional should yield the two functions $\vartheta(r)$ and $\varphi(r)$ which describe the true nature of the incommensurate surface structures [such as those of Mo(001) or W(001):H].[62] With the additional assumption $\varphi=\text{const}=n\pi$, one recovers the simpler commensurate-incommensurate Hamiltonian leading to a soliton lattice,[61] as already mentioned. Conversely, if we set $\vartheta=(2n+1)\pi/2$, as would be appropriate for $\Delta\to\infty$ (when the z degree of freedom drops out) then we trivially recover the M_5 commensurate Hamiltonian Eq. (9), involving x-y motions only.

Though we have been able to find no existing study of the full problem of minimizing $\Delta E(\vartheta,\varphi)$ of Eq. (14) in the literature, we see several reasons why this should be very interesting. The first is the physical consideration that the detailed form of the discommensurations separating regions ("stripes") of predominant u character ($\vartheta\sim\pi/2$, $\varphi=0$) from regions of predominant v character ($\vartheta\sim 0$) will certainly be greatly affected by acquiring some $\bar{u}$ admixture (i.e., by allowing $\varphi\neq 0$ in the discommensuration region). The second, more general consideration is that minimization of Eq. (14) corresponds formally to a dynamical Hamiltonian problem where the number of phase space variables $(\vartheta,\nabla\vartheta,\varphi,\nabla\varphi)$ exceeds three. Such problems with a large number of variables may be expected to yield quasiperiodic, or chaotic behavior, rather than periodic behavior.[63] This leads to the rather suggestive possibility that some incommensurate surface reconstructions could be described by nontrivial nonperiodic distortions, which nevertheless are in a sense "ordered." On the experimental side, this would probably show up as some apparent disorder, and "streaking" in the LEED and He diffraction patterns. We hope to come back in the future to discussing this interesting possibility more closely.

VI. EFFECTS OF RELAXATION AND LGH PARAMETERS OF THE $c(2\times2)\langle 11\rangle$ PHASE OF W(001)

The ("Debe-King") $c(2\times2)\langle 11\rangle$ distortion of W(001) stems, in our description, from an M_5 instability. As such, it is described in principle by the LGH Eq. (9). If, however, one wants to tie quantitatively such an expansion with the actual microscopic energetics of W(001) discussed in the previous section, then some slight extension is needed. This need stems from two facts: (i) The surface relaxation parameter h which we have found in Sec. IV to be quantitatively important, has to be included; (ii) if the vertical (M_1-type) displacements (though not present in the static mean-field distortion) were actually not too far from being unstable, their presence could not in principle be neglected. In some respects, this problem is analogous to that of including the $\bar{u}$ degrees of freedom in addition to (u,v) in the incommensurate problem discussed in the preceding section. In fact, the Hamiltonian we consider has the same form as Eq. (14), plus a relaxation term

$$\begin{aligned}\Delta E=\int d^2x\{&-r(u^2+\bar{u}^2+v^2)+a(u^2+\bar{u}^2+v^2)^2+\Delta v^2+Av^4+bu^2\bar{u}^2+b_1(u^2+\bar{u}^2)v^2\\&-c_1h(u^2+\bar{u}^2)-c_2hv+\mu h^2+\text{gradients}\}\ .\end{aligned}\tag{15}$$

In the $c(2\times2)\langle 11\rangle$ state, b is <0, and the $T=0$ mean value of the order parameter is characterized by $\langle u\rangle=\langle\bar{u}\rangle=\rho_0/\sqrt{2}\neq 0$, $\langle v\rangle=0$, or $\rho_0=\langle[(u^2+\bar{u}^2)]^{1/2}\rangle$ (for $r>0$ and Δ sufficiently large). Moreover, a finite relaxation $h_0=\langle h\rangle\neq 0$ will accompany the reconstruction.

Mean-field minimization of Eq. (15) yields $\partial\Delta E/\partial\rho^2=0$, $\partial\Delta E/\partial h=0$, whose solution is the following:

$$\rho_0^2=\frac{r}{2a-|b|/2-c_1^2/2\mu}\tag{16}$$

and

$$h_0 = c_1^2 \rho_0^2 / 2\mu \ . \tag{17}$$

This result shows the following.

(a) Both the in-plane distortion and the vertical relaxation are proportional to the "driving" parameter r. This quantity is identified with the squared frequency of the "fastest growing" M_5 mode $-r = M\omega_5^2/2$.

(b) The effect of the anharmonic term $(a - |b|/4)$ is, as expected, to block the growth of the distortion.

(c) The inclusion of relaxation ($h_0 \neq 0$) favors the increase of the distortion, as already found in our energy minimization of Sec. IV. Incidently, this implies values of $c_1^2/2\mu$ small enough in comparison with $2a - |b|/2$, which is a critical value. Close to and beyond this value the fourth order expansion Eq. (15) is no longer sufficient.

(d) The outwards accompanying relaxation ($h_0 > 0$) found in Sec. IV can be accounted for by a positive sign of the LGH parameter c_1.

The presence of 4 degrees of freedom in the starting LGH Eq. (15) implies that ΔE is a positive quadratic form of the four small amplitudes $u - \langle u \rangle$, $\bar{u} - \langle \bar{u} \rangle$, v, and $h - \langle h \rangle$. Leaving aside h which is not a normal coordinate and whose "spring constant" μ remains unchanged, the remaining 3 degrees of freedom lead to the corresponding vibration frequencies

$$\omega_l^2 = 4r \left[1 + \frac{c_1^2/2\mu}{2(a - |b|/4) - c_1^2/2\mu} \right] \quad (\langle 110 \rangle \text{ motion}) \ ,$$

$$\omega_T^2 = \frac{|b| r}{a - |b|/4 - c_1^2/2\mu} \quad (\langle 1\bar{1}0 \rangle \text{ motion}) \ , \tag{18}$$

$$\omega_Z^2 = 2[-r + \Delta + (2a + b_1)\rho_0^2 - c_2 h_0] \quad (\langle 001 \rangle \text{ motion}) \ .$$

These three frequencies ω_L, ω_T, and ω_Z, have a straightforward lattice vibration correspondence. By looking at the eigenvector in Eq. (18) we identify ω_L as a longitudinal in-plane "amplitude" mode, and ω_T as a transverse (or more correctly, shear horizontal) "phase" mode. The amplitude mode frequency is directly proportional to the unstable frequency $\omega_5^2 = -2r/M$, and has to do with the overall stability of the $c(2\times2)$ distortion against modulation of the amplitude ρ_0. The phase mode ω_T, on the other hand, is connected with the relative stability of the $\langle 11 \rangle$ distortion relative to the $\langle 10 \rangle$. Its frequency therefore vanishes, together with the LGH parameter b, at the dividing line, shown in Sec. IV (Fig. 7), between $\langle 11 \rangle$ and $\langle 10 \rangle$. The overall effect of surface relaxation is to improve stability, and to push both ω_L and ω_T up, corresponding to the larger distortion Eq. (16), and to some extra energy gain.

Finally, the vertical vibration frequency ω_Z represents simply the translation to the $c(2\times2)$ surface of the M_1 mode of the ideal surface, upshifted by the M_5 distortion, through the anharmonic coupling a and b, and downshifted by the outwards relaxation, through c_2.

Given the microscopic Hamiltonian and parameters ($\alpha_s = -0.75$ eV/Å^2, $\beta_s = -0.94$ eV/Å^2, $\gamma_s = 3.76$ eV/Å^2, $\delta_s = 225.67$ eV/Å^2) given in Sec. IV, we can and have, by identifying the results of the two approaches, determined the values of the $T=0$ LGH parameters of W(001). They are given in Table II.

TABLE II. Numerical values of the LGH parameters for W(001)$c(2\times2)$ at $T=0$ given in Eq. (13).

r (eV/Å^2)	a (eV/Å^4)	Δ (eV/Å^2)	A (eV/Å^4)	b (eV/Å^4)
1.20	16.1	2.44	8.9	−10.6
b_1 (eV/Å^4)	c_1 (eV/Å^3)	c_2 (eV/Å^3)	μ (eV/Å^2)	
−7.3	5.5	16.5	4.05	

VII. SURFACE PHONONS OF CLEAN W(001)

Starting with our lattice Hamiltonian Eq. (2), with the effective potential surface parameters and static $T=0$ distortion as in Sec. IV, it is straightforward to generate a (001) slab with two statically distorted surfaces, and to recalculate the full reconstructed surface phonon spectrum, over the new 2D Brillouin zone.

The $c(2\times2)\langle 11 \rangle$ surface has C_{2v} symmetry, where obviously the $\langle 11 \rangle$ and $\langle 1, -1 \rangle$ directions—previously equivalent on the undistorted surface (C_{4v})—are now inequivalent. In particular, this new structure has a glide plane, which causes modes to stick together in pairs[64] at $(\frac{1}{4}, -\frac{1}{4})2\pi/a_0$.

In our calculation we have statically displaced only the first-layer atoms away from the ideal positions according to the M_5 eigenvector (purely in-plane) with a distortion amplitude ρ_0. We have neglected for simplicity the distortion on the second layer. That distortion can be estimated to be about $\frac{1}{4}$ of the distortion on the first layer.[27,44,42] However, the corresponding corrections to the surface energetics are only of second order, and thus very small.

We present the phonon spectra calculated in this way in Fig. 9. We note the following.

(i) Besides the normal "bulk continua" there are in this spectrum several surface modes, and/or strong surface resonances. Most of them lie within or below the bulk continua, but there are also modes pushed up *above* the bulk continuum.

(ii) There are generally six surface modes of rather mixed polarization corresponding to two atoms in the unit surface cell.

(iii) In particular, three modes emerge as strong surface resonances at $q=0$. These modes can be identified with $\omega_L, \omega_T, \omega_Z$, of the simple Landau-Ginsburg (LG) picture in the previous section.

For easy reference, and in order to help understanding how much the reconstruction distortion has changed the surface phonon spectra, we present in Fig. 10 also the hypothetical phonon spectra of the undistorted W(001), taken with surface force constants equal to the bulk, namely $(\alpha_s, \beta_s, \gamma_s, \delta_s) = (\alpha_2, \beta_2, \gamma_2, \delta_2)$, but folded into the $c(2\times2)$ Brillouin zone. We note that, the truly distorted $c(2\times2)$ surface has many more low-frequency surface modes, particularly modes with an in-plane component. In Fig. 11 we illustrate some of the eigenvectors of these modes.

At high frequencies, where the unreconstructed surface

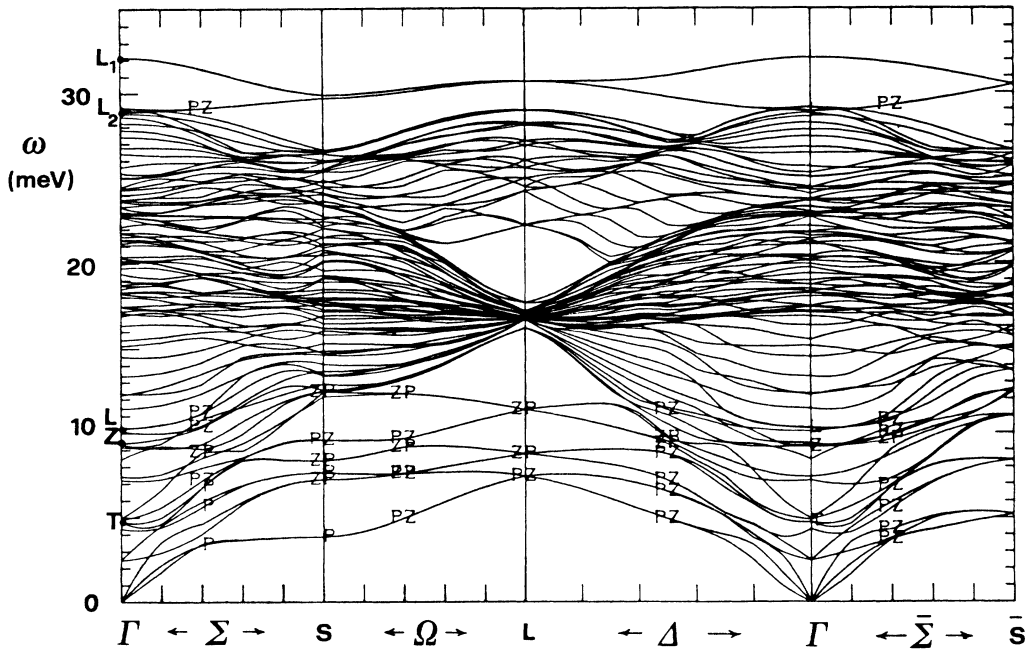

FIG. 9. Phonon spectrum of the W(001)$c(2\times2)\langle 11\rangle$ reconstructed surface calculated with the parameters of the point P ($\alpha_s=-0.75$ eV/Å^2, $\beta_s=-0.94$ eV/Å^2, $\gamma_s=3.76$ eV/Å^2, $\delta_s=225.67$ eV/Å^2) and 15 layers. Modes which have a squared first-layer component of the (normalized) eigenvector $>30\%$ are marked according to their main polarization (P=planar, Z=vertical). At the Γ point the polarizations of modes labeled L (longitudinal) and Z (vertical) is in reality of mixed character. L or Z simply indicates the main component. The T mode is instead strictly shear horizontal. These three modes L, Z, and T correspond to the three frequencies ω_L, ω_T, and ω_Z (see text).

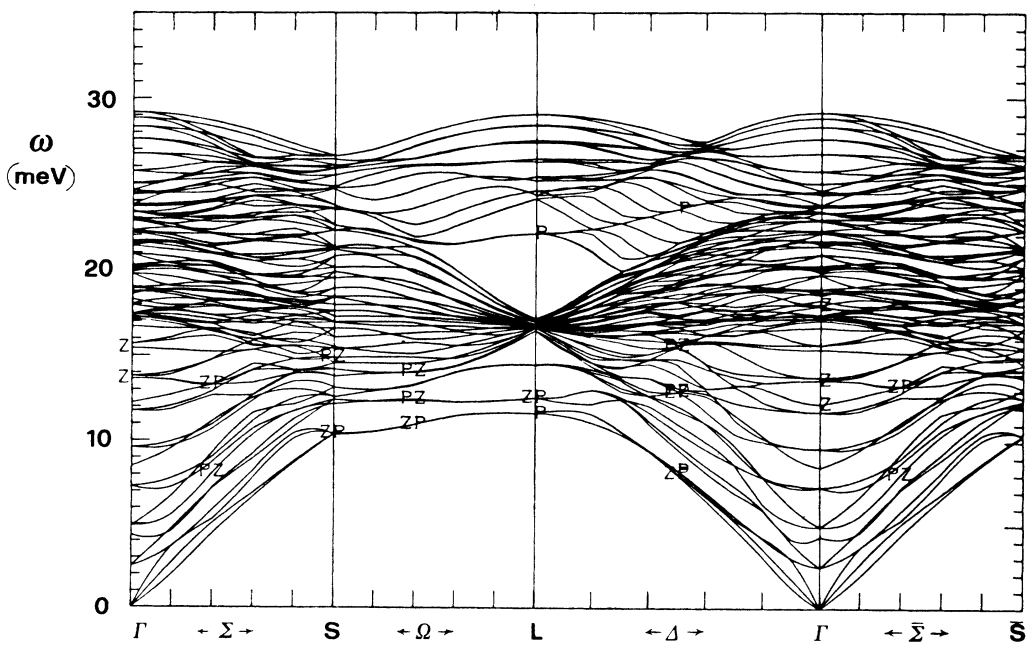

FIG. 10. Phonon spectrum of the ideal surface (with bulk force constants) folded into the BZ of the reconstructed surface. Modes with a squared first-layer component $>30\%$ are marked. Here at the Γ-point longitudinal and vertical modes have different symmetry. This figure serves to demonstrate, when compared with the true phonon spectrum of Fig. 9, how large and important are the changes brought about by reconstruction.

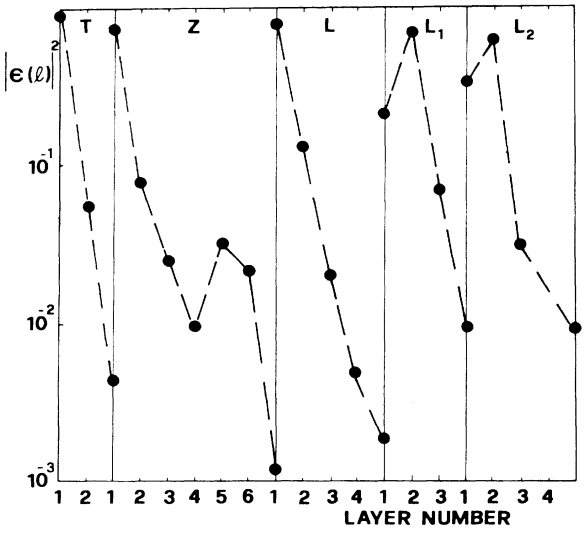

FIG. 11. Square distortion amplitude of the surface mode eigenvector as a function of the depth (surface $l=1$) for the five modes with surface character at the Γ point.

has no special modes we find two split-off modes on the reconstructed surface labeled as L_1 and L_2. They can generally be attributed to an effect of strain exerted on the second layer by the first-layer distortion. This is confirmed by looking at the eigenvectors of these high-lying modes (represented in Fig. 11) which are indeed large on the second layer.

From the surface phonon spectrum of Fig. 9 we also extract a crude value for the phase coherence length in the form $\xi^{\text{phase}} \sim 2\pi/\delta q$, with $\delta q = 2\pi\omega_T/s$. Here, ω_T is the phase mode frequency (here 4.7 meV), and s describes its dispersion along Σ, taken as $(\omega_T^2 + s^2 q^2)^{1/2}$. This yields $\xi^{\text{phase}} \sim 12$ Å, compatible with experiments.[52,4,5,27] The results established in the present chapter constitute a precise theoretical prediction for the low-temperature surface vibrations of clean reconstructed W(001). As of this date, there is very little experimental evidence to be used for comparison. Inelastic electron scattering experiments have been reported,[65] which however lack of resolution at low-energy loss, $\omega < 20$ meV, where most of our calculated features lie. One peak has been reported at 36 meV, which could be tentatively identified with our mode L_1. Its eigenvector is about 50% in-plane longitudinal (the two surface atoms out of phase) and 50% vertical (the two surface atoms moving in phase). The amplitude is about twice as much in the second layer than in the first. All atoms in the first layer move vertically bodily together, and so do all atoms on the second layer. However, the two layers are 180° out of phase; i.e., they vibrate one against the other. Further work on the expected temperature dependence of this and other modes is in progress.

VIII. DISCUSSION AND CONCLUSIONS

We have presented in this paper a theory of the reconstructed W(001)$c(2\times2)$ clean surface. The theory is based on a phenomenological effective lattice Hamiltonian, characterized by an adjustable surface interatomic potential specified by four parameters $\alpha_s, \beta_s, \gamma_s, \delta_s$. We have shown how in this theory the unreconstructed surface becomes unstable, and how to describe the new stable reconstructed surface, in a quantitative way at $T=0$. Known experimental quantities, such as the distortion magnitude and the coherence length help us to choose the adjustable parameters, although they do not really specify them uniquely. Nevertheless, the most important findings do not depend critically upon fine details of the parametrization chosen. Thus, for example, we expect quite generally that the reconstruction should involve an energy of some 30 meV per surface atom, and that the reconstructed surface should be about 2% outwards relaxed with respect to the (unstable) unreconstructed surface.

While our statements are valid at $T=0$, they should not be taken to imply that at the reconstruction phase transition of W(001) (which occurs near room temperature) there should be a 2% inwards relaxation, or an energy increase of 30 meV. One might rather expect, based also on our phonon results to be discussed in a moment, that at T_c the *phase* of the order parameter is lost, rather than the amplitude. In that case, a short-range distortion would be present also above T_c, except that long-range coherence would be lost. If that were the situation, then the surface relaxation and the energy gain just discussed would be only marginally affected at T_c. In contrast to this, an energy gain upon reconstruction of only 10 meV/surface atom or less would seem reconcilable with a T_c of 200–300 K only if the distortion *magnitude* become negligible above T_c.

Coming back to $T=0$, we have then calculated the surface phonon spectrum of the reconstructed W(001)$c(2\times2)\langle 11\rangle$ surface. Our results show that the reconstructed surface exhibits a wealth of new specific surface vibrations, which should be readily observable with current experimental techniques (particularly He and inelastic electron scattering). In particular, one mode at 36 meV reported in the literature[65] may be connected with our mode L_1.

As an additional useful tool, we have discussed Landau-Ginzburg Hamiltonians for the surface reconstruction of W(001) [and of the closely related Mo(001)]. These Hamiltonians help to establish a simple approximate connection between the surface static distortion and its dynamics (i.e., $q=0$ surface phonons) which in principle goes beyond our lattice Hamiltonian model. Future measurements of surface vibrations of this and other surfaces may thereby be directly related to the $T=0$ surface energetics through such Hamiltonians. The LGH for incommensurate reconstructions such as that of Mo(001) or of W(001):H, is presented and intriguing possibilities connected with it are pointed out.

Before closing, we wish to speculate again briefly on the implications of our $T=0$ results on the surface phase transition, as well as on the possible temperature behavior of surface phonons.

As the energetics of Sec. IV and the LGH Eq. (15) of Sec. VI shows, it is really energetically very costly to try to change the reconstruction amplitude ρ_0, but it is instead

very easy to change its phase, e.g., from ⟨11⟩ to ⟨10⟩. This implies that with temperature a strong anharmonic shift (and broadening) could build up, affecting mostly the shear horizontal ω_T mode. We are thus led to speculate that, to some extent, this phonon could exhibit some softening, at least well below T_c (where quasiharmonic behavior may still hold). We have calculated tentatively the change of ω_T upon decreasing very slightly the distortion amplitude from its equilibrium value (all of this at $T=0$, however). We find that decreasing ρ_0 from $0.22 \rightarrow 0.19$ Å is sufficient to drop ω_T from 5 meV to zero. It may be expected that the effect of temperature could result in a softening (as well as a broadening) of ω_T, at least at low T. The amplitude mode ω_L, which is connected with the reconstruction magnitude is not expected to soften initially quite as much as ω_T. However, it should then soften quite dramatically near the transition temperature, because it must coincide with ω_T at high temperatures where the surface recovers the full C_{4v} symmetry. In this case ω_L,ω_T become degenerate partners of ω_5. We hope to return to these questions in the near future.

ACKNOWLEDGMENTS

We are grateful to G. Santoro for cooperation in earlier stages of this project. We are especially indebted to C. Z. Wang and M. Parrinello for useful discussions and also for helping us to test with molecular dynamics a better bulk potential parametrization of W.

APPENDIX A: INSTABILITIES OF THE IDEAL SURFACE

By continuously varying the harmonic SFC α_s,β_s and looking for surface instabilities ($\omega^2<0$) we can construct the stability diagram of Fig. 3. Regions of α_s,β_s where all modes are real correspond to a stable undistorted (1×1) surface. The point $\alpha_s=\alpha_2$, $\beta_s=\beta_2$ obviously belong in this region. The corresponding phonon spectrum is shown in Fig. 12. When, however, α_s,β_s are drastically changed from their bulk values, one or more surface phonon frequencies may go imaginary. Then, as explained in Sec. III we expect a reconstruction, obtained by "freezing in" a distortion proportional to the eigenvector of the fastest growing mode. Within this harmonic scheme, we obtain, besides the region of ideal surface stability, five separate regions of instability. Each of them is labeled in Fig. 3 by the type of its soft mode. Three of these five types of instability occur at the high-symmetry points $M=(1/2,1/2)2\pi/a_0$ or $L=(1/2,0)2\pi/a_0$. They give rise to three types of commensurate reconstructions, namely M_1,M_5,L_2. Typical unstable surface phonon spectra for each of these regions are those of Figs. 13, 14, and 15. The two remaining instabilities I_1 and I_2 occur in the neighborhood of either M or L. They give rise to incommensurate reconstructions discussed further below in Appendix B. In Fig. 3 we conventionally draw lines between the stable region and the others at the point where the corresponding phonon frequency vanishes $\omega^2_{q,\lambda}=0$. It is more difficult to trace dividing lines between the unstable regions. Often, in fact, more than one phonon frequency is imaginary and it is not clear which reconstruction prevails. In that case, the actual reconstruction depends in principle also on the anharmonic forces that act to limit the growth of each possible reconstruction. These anharmonic forces are generally not the same for two different surface phonons. Nevertheless, we have decided for simplicity to stick to the harmonic picture and simply as-

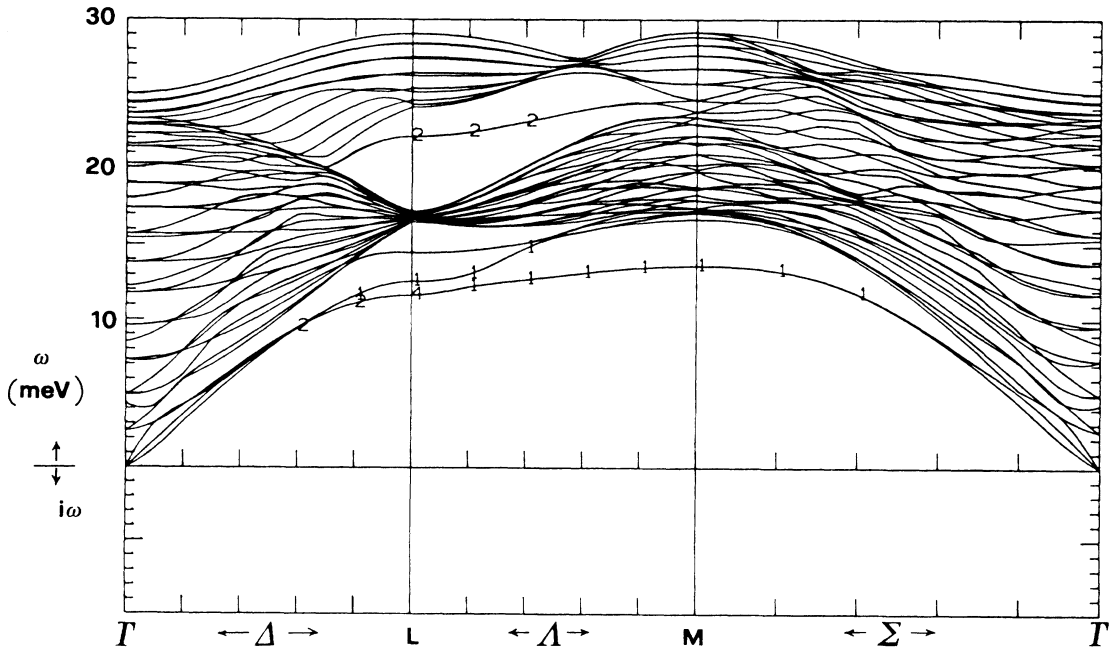

FIG. 12. Phonon spectrum of the ideal 1×1 surface with $\alpha_s=\alpha_2$, $\beta_s=\beta_2$. The symmetry labels mean 1=even, 2=odd along symmetry lines, and correspond to labels of C_{4v} at Γ, L, and M [notation of Koster, Dimmock, Wheeler, and Statz (Ref. 68)].

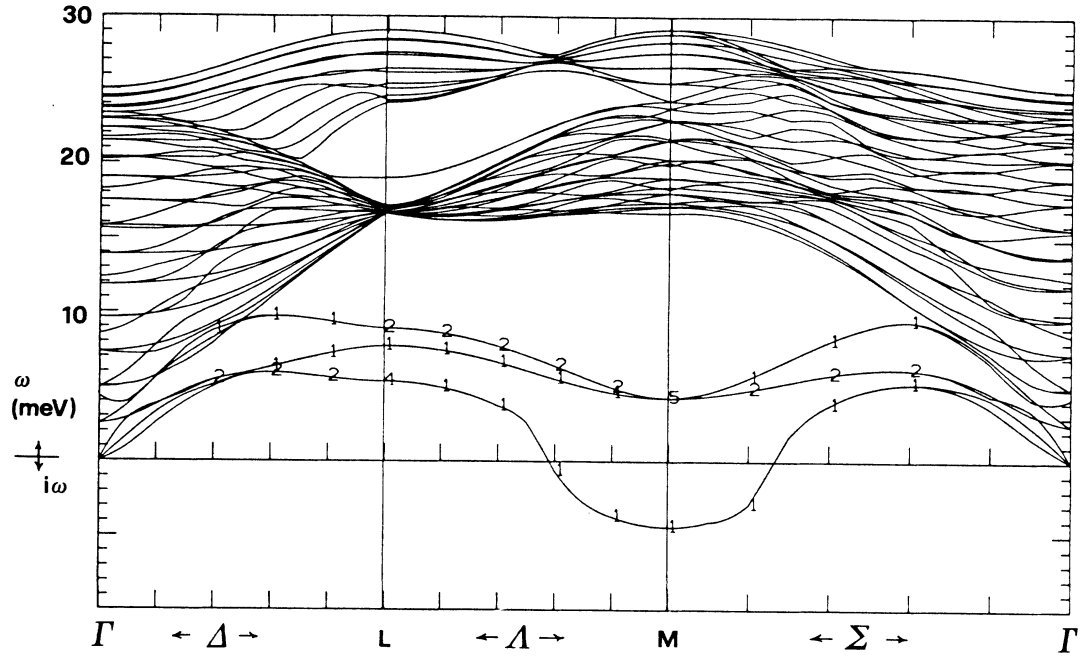

FIG. 13. Phonon spectrum of the ideal surface with $\alpha_s = -1.2$ eV/Å^2, $\beta_s = -0.3$ eV/Å^2 inside the M_1 region.

sume that the phonon with lowest ω^2 will prevail.

The M_1 surface phonon involves displacements normal to the surface, i.e., with **u** along $\langle 001 \rangle$. The eigenvector is similar to that of M_5 given in Eq. (7), except for $\hat{z}$ replacing $(\hat{x}+\hat{y})$. The corresponding reconstruction consists of a raising and lowering of alternate chains, leading to a $c(2\times2)$ unit cell.

The M_5 surface mode is twofold degenerate with **u** along $\langle 110 \rangle$ or $\langle 1\bar{1}0 \rangle$, leading to a $c(2\times2)$ unit cell. The clean surface reconstruction (Debe-King model) corresponds to a frozen-in mode as given by Eq. (7). Only one of the two components of the displacement is dif-

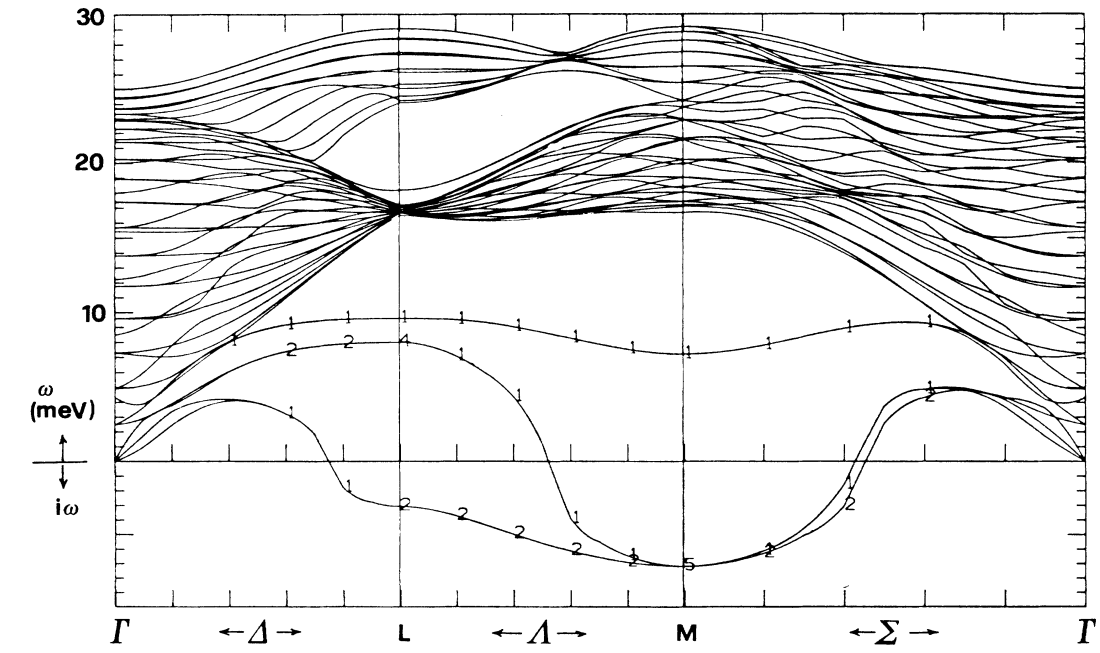

FIG. 14. Phonon spectrum of the ideal surface with $\alpha_s = -0.75$ eV/Å^2, $\beta_s = -0.94$ eV/Å^2 corresponding to the point P inside the M_5 region.

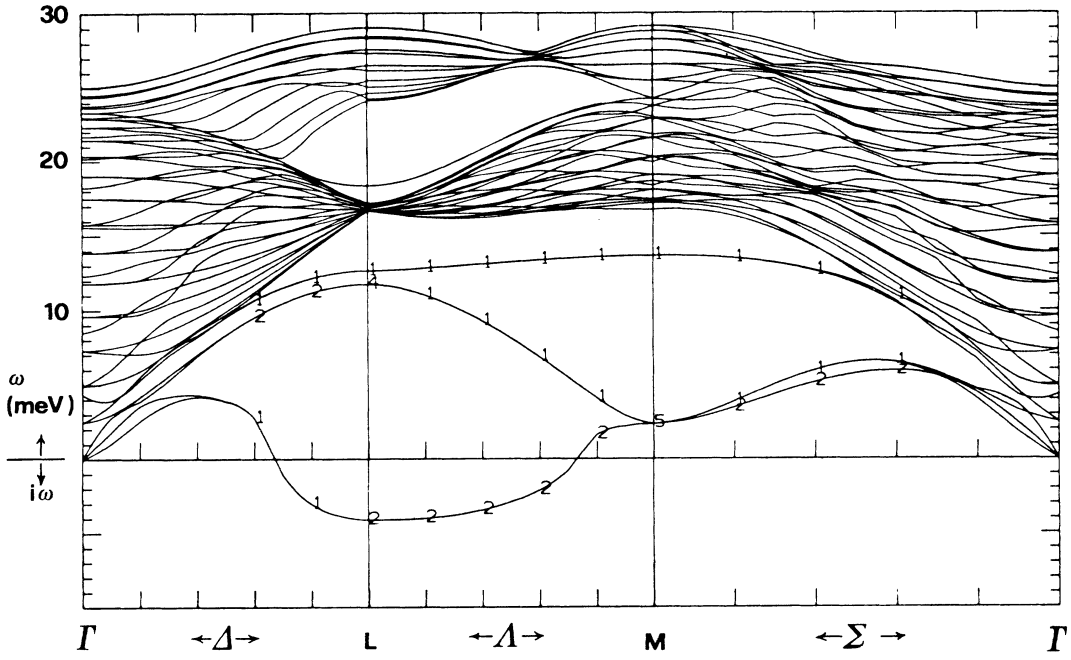

FIG. 15. Phonon spectrum of the ideal surface with $\alpha_s = -0.0$ eV/Å^2, $\beta_s = -1.05$ eV/Å^2 inside the L_2 region.

ferent from zero, giving rise to two possible domains oriented along $\langle 110 \rangle$ and $\langle 1\bar{1}0 \rangle$. We call this a $c(2\times2)\langle 11 \rangle$ reconstruction. However, depending on anharmonic terms (see also Sec. V), a different situation can occur where both $\langle 110 \rangle$ and $\langle 1\bar{1}0 \rangle$ components of the displacement are different from zero and equal in magnitude. Then we have a different reconstruction, which we call $c(2\times2)\langle 10 \rangle$. This too has two possible types of domains with displacements along either $\langle 100 \rangle$ or $\langle 010 \rangle$. A $c(2\times2)\langle 10 \rangle$ reconstruction seems to take place when a small amount of hydrogen is deposited on W(001).[4,50,51]

Finally, we discuss the L_2 reconstruction. There are two degenerate inequivalent L points, namely $(1/2,0)2\pi/a_0$ and $(0,1/2)2\pi/a_0$. The corresponding L_2 eigenvectors point along $\langle 100 \rangle$ and $\langle 010 \rangle$, respectively. Condensation of one of them alone leads to a (2×1) reconstruction. Simultaneous condensation of both, on the other hand, produces a (2×2) phase. Again, the anharmonic terms decide between the two possibilities. Neither of these reconstructions has ever been reported on this type of surfaces.

APPENDIX B: INCOMMENSURATE SURFACE PHASES *I*1 AND *I*2

For special ranges of the surface force constants α_s and β_s falling at borderline values between those yielding an M_5 instability and either an M_1 (for the case of I_1) or an L_2 (for the case of I_2) instability, the phase diagram of Fig. 3 in Sec. III indicates the tendency toward the *incommensurate phases* I_1 and I_2. As discussed, in this Appendix, we describe (a) how this indication is obtained, (b) the physical mechanism underlying this tendency to incommensurability, and (c) the type of distortion to be eventually expected in such a phase, at least at $T=0$.

A. Commensurate and incommensurate instability

For a start, let us consider on Figs. 12, 13, 14, and 15 the slab phonon spectra characteristic of an ideal (i.e., unreconstructed) W(001) surface which is either stable (when α_s,β_s take the unperturbed bulk values) or exhibits M_1, M_5, or L_2 commensurate instabilities, respectively. At these commensurate instabilities the fastest growing mode is a zone boundary mode, indicating a tendency to form various commensurate reconstructions, such as $c(2\times2)$, or (2×2) or (2×1), as discussed in Appendix A.

However, it is also possible to find an instability at a k vector $\mathbf{q}_0$ slightly away from the zone boundary. Of course, when this happens, the fastest growing mode is incommensurate with the ideal surface lattice. The way in which this occurs in region I_1 and I_2 is shown in Figs. 16 and 17, respectively. In both spectra the fastest growing mode, indicated by an arrow, occurs not at M but some deviation $\delta\mathbf{q}$ away. Quantitatively, the imaginary phonon frequency at the incommensurate point is only marginally, often imperceptibly, better than at the M point. This fact indicates that, within the limits of a linear analysis, the energetic extra benefit to be expected from driving the reconstruction incommensurate does exist, but will never be very large. We will come back to an important consequence of this marginality. The deviation $\delta\mathbf{q}$ (the inverse of a wavelength which corresponds to the "beat" between the best reconstruction wavelength $2\pi/|\mathbf{q}_M+\delta\mathbf{q}|$ and

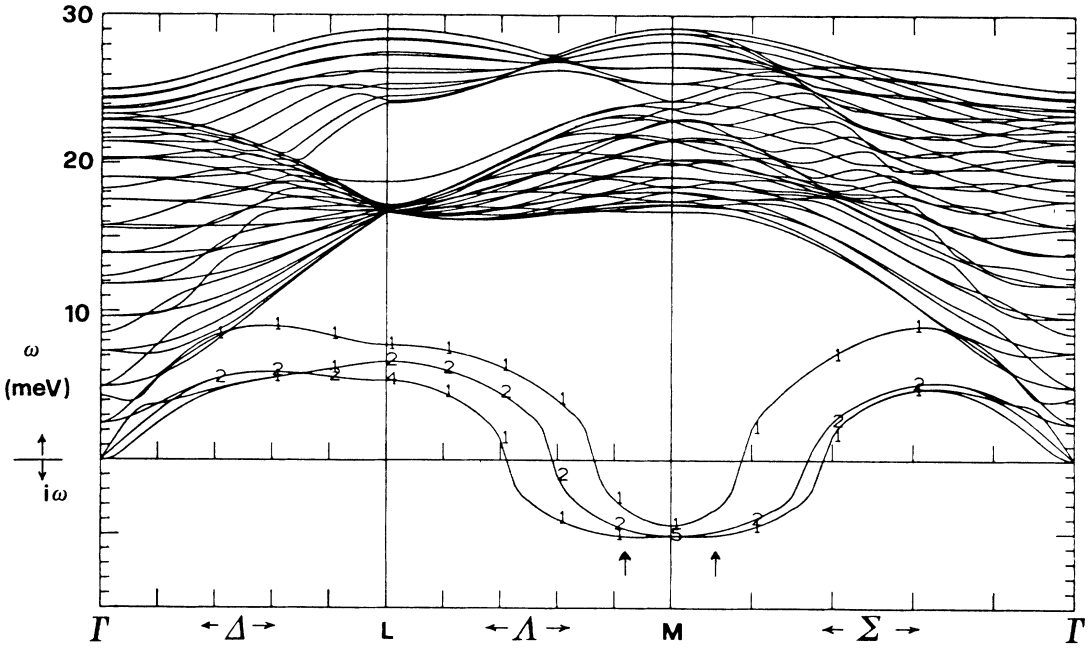

FIG. 16. Phonon spectrum of the ideal surface with $\alpha_s = -1.2$ eV/Å^2, $\beta_s = -0.23$ eV/Å^2 inside the incommensurate region I_1. The arrows denote fastest growing modes for the resulting incommensurate phase.

the commensurate M-point wavelength $2\pi/|\mathbf{q}_M|$ behaves quite differently in I_1 and I_2. On crossing the region I_1, e.g., by moving on the phase diagram of Fig. 3, the deviation $\delta\mathbf{q}$ starts from zero at the boundary M_5-I_1, grows to rather small values ($\delta\mathbf{q}_{\max}/\mathbf{q}_M \lesssim 10\%$) and returns to zero again at the boundary I_1-M_1. On the other hand, as one crosses the region I_2, the deviation $|\delta\mathbf{q}|$ starts from zero at the boundary M_5-I_2, grows rapidly, and settles to $|\delta\mathbf{q}| = \pi/a_0 = |\mathbf{q}_M - \mathbf{q}_L|$ at the boundary I_2-L_2.

B. Physical mechanism

The mechanism leading to incommensurability of the displacively distorted surfaces can be given several levels of description. Furthermore, it is different for the two

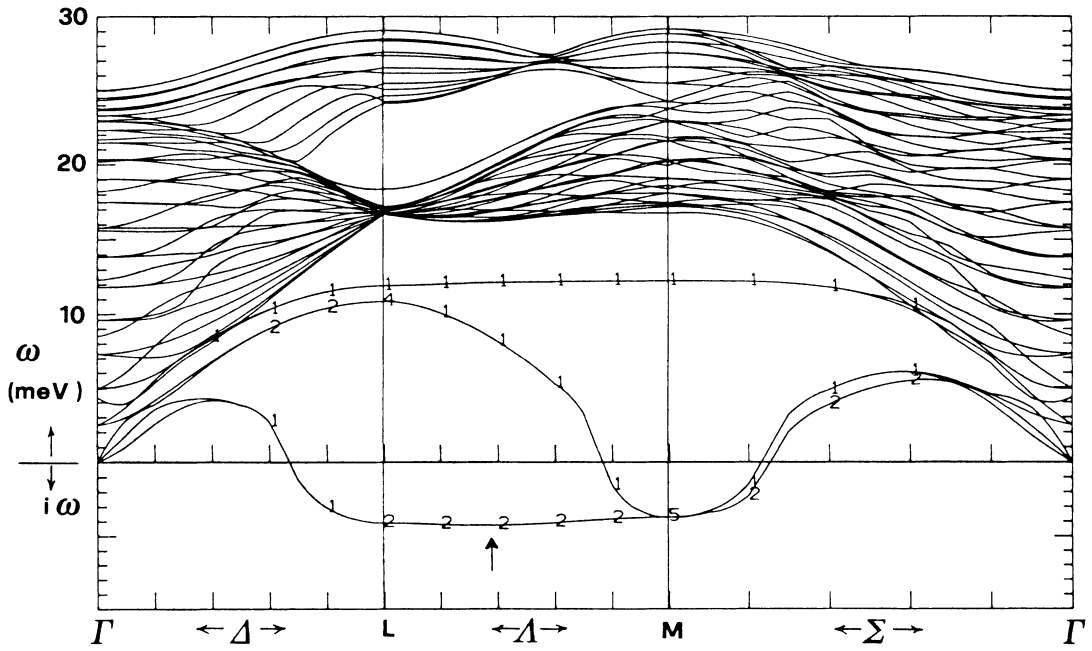

FIG. 17. Phonon spectrum of the ideal surface with $\alpha_s = -0.23$ eV/Å^2, $\beta_s = -1.05$ eV/Å^2 inside the I_2 region.

phases I_1 and I_2. We begin with I_1, which is both more interesting physically, and more important since it has immediate realizations, such as the clean reconstruction of Mo(001). A first level of description is in terms of coupling between soft phonon modes of different symmetry. Incommensurability of type I_1 arises when the two different soft modes—the planar M_5 mode and the vertical M_1 mode—are both unstable and very close in (imaginary) frequency. If they could mix, one of the two mixed modes would end up being lowest. Symmetry, of course, prevents mixing at the M point. However, mixing becomes allowed away from the M point, where the symmetry is lowered. For $\delta\mathbf{q}$ along either $\langle 11\rangle$ or $\langle 10\rangle$, the M_1-compatible mode and one member of the twofold degenerate M_5-compatible modes have same symmetry. As the M_1 and M_5 frequencies cross each other this leads to a range where the lowest mode is incommensurate as on Fig. 18. Schematically, the corresponding dynamical matrix can be written as

$$\underline{D}(q)=\begin{bmatrix} \omega_1^2+J_1\,|\,\delta\mathbf{q}\,|^2 & is\,|\,\delta\mathbf{q}\,| \\ -is\,|\,\delta\mathbf{q}\,| & \omega_5^2+J_5\,|\,\delta\mathbf{q}\,|^2 \end{bmatrix}, \tag{B1}$$

where J_1 and J_5 phenomenologically describe the two dispersions, and s their coupling. The coupling is pure imaginary, so that the M_1 and M_5 components of the mixed mode are in quadrature,[66] rather than in phase.

At the next level, we can go back to the diagram of Fig. 3 and select in it a point in the M_5 region, and consider that by merely decreasing α_s one can enter the I_1 incommensurate region, to end up in the M_1 region. A decrease of α_s amounts to an increasing repulsion between first surface-neighbor atoms. A look at the diagram of Fig. 6 makes it clear why one should go from M_5 to M_1, in terms of purely *top layer* atom-atom distances. The necessity of an intermediate incommensurate phase, however, cannot be understood without including the second atomic layer. It is easy to check, for example by using the effective mass method of Fasolino, Santoro, and Tosatti[44] that the $is\,|\,\delta\mathbf{q}\,|$ coupling term leading to incommensurability is entirely due to second-layer coupling. Incommensurability, here as elsewhere, comes about as a sort of compromise between competing forces, pushing for different structures. Here, the top-layer forces would suddenly like to switch, as α_s decreases, from M_5, planar, to M_1, vertical, distortions. However, planar distortions bother the second layer a lot less than vertical distortions. These have the undesirable feature of causing a clash of atom cores between the two layers, which causes a competition to occur.

Perhaps the ultimate level of physical description of the necessity of I_1 incommensurability on a bcc (001) surface can be reached by abandoning sinusoidal phononlike distortions and going straight over to sharp boundaries, as done for the case of ferroelectrics by Heine and McConnell.[66] Suppose we consider an M_5 distortion, with an antiphase boundary, as in Fig. 19. Then, it is immediate to see that the first-layer atoms at the boundary are pushed by the concurrent motion of the second layer, alternatively up, or down. This illustrates how, generally allowing a phase slip of an M_5 distortion, a local M_1 parasite distortion naturally creeps in. As in Heine and McConnell case,[66] steric hindrance arguments are fully sufficient to understand this coupling. This completes our discussion of the physical motivations for the existence of the I_1 phase.

We have much less to say about I_2. The difference between Figs. 16 and 17 makes it very clear that the incommensurate I_2 phase arises in a rather different way from I_1. If we restrict ourselves to the lowest three surface

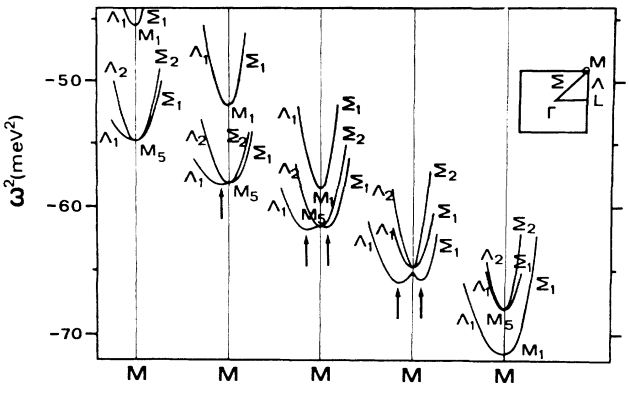

FIG. 18. Sketch of the mechanism leading to incommensurability in the I_1 region. The modes M_1 and M_5 are orthogonal at the M point, but interact away from the M point, both along the Σ and the Λ lines. The doublet of interacting Σ_1 and Λ_1 modes gives rise to minima away from the M point when the M_1 and M_5 frequencies cross. From Ref. 28.

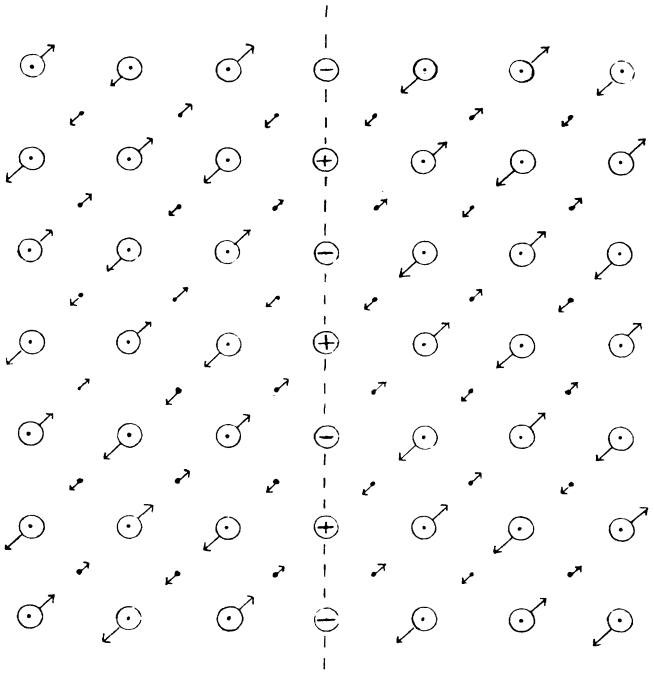

FIG. 19. Aspect of the surface with an M_5 distortion and an antiphase boundary. Open circles denote first-layer atoms, small dots second-layer atoms.

phonons, there appears no clear reason for incommensurability. The very shallow incommensurate minimum apparently arises via coupling through bulk modes and resonances. Unlike the case of I_1, straight consideration of the first two layers, and of steric hindrance between them, does not suffice to explain incommensurability. We leave here the issue at this point; it is clear that the higher level of practical complication called for to understand I_2 can be handled along similar lines as I_1, should it be desirable in the future.

C. Incommensurate distortion

We finally come, before closing this Appendix, to a brief discussion of the type of $T=0$ distortion to be expected of surface displacive incommensurate phases, such as I_1 and I_2. Quite generally, this distortion will be such as to minimize a suitable energy functional, such as Eqs. (9)—(15), or one of those discussed by Bak,[60] if a single-phase approximation is good enough. Like that case, the minimum to be expected is of soliton-lattice type, i.e., an array of domains of approximately commensurate areas, separated by solitons, or walls or boundaries, roughly like that of Fig. 19. These walls, in general have a finite width, rather than an abrupt nature, as in that figure. The actual width of the wall relative to the domain size is a quantity which depends critically upon the system parameters. In our case, we can argue that the width of domain walls should be substantially smaller than the domain size. It was pointed out earlier that the energy difference can only naturally be accommodated with a sharp soliton lattice, where the "misfit" region is very localized, and essentially all the incommensurate surface is identical with the commensurate case.

[1]T. E. Felter, R. A. Barker, and P. J. Estrup, Phys. Rev. Lett. **38**, 1138 (1977).

[2]M. K. Debe and D. A. King, J. Phys. C **10**, L303 (1977).

[3]For a review see Roy F. Willis, in *Dynamical Phenomena at Surfaces, Interfaces and Superlattices,* edited by F. Nizzoli, K. H. Rieder, and R. F. Willis (Springer, Berlin, 1985), p. 126.

[4]R. A. Barker and P. J. Estrup, J. Chem. Phys. **74**, 1442 (1981).

[5]D. A. King and G. Thomas, Surf. Sci. **92**, 201 (1980).

[6]D. A. King, Phys. Scr. T **4**, 34 (1983).

[7]E. Tosatti, Solid State Commun. **25**, 637 (1978).

[8]J. E. Inglesfield, J. Phys. C **11**, L69 (1978); **12**, 149 (1979).

[9]K. Terakura, I. Terakura, and Y. Teraoka, Surf. Sci. **86**, 535 (1979).

[10]K. Terakura, I. Terakura, and N. Hamada, Surf. Sci. **103**, 103 (1981).

[11]H. Krakauer, M. Posternak, and A. J. Freeman, Phys. Rev. Lett. **43**, 1885 (1979).

[12]M. Posternak, H. Krakauer, and D. D. Koelling, Phys. Rev. B **21**, 5601 (1980); **30**, 4828(E) (1984).

[13]C. L. Fu, S. O. Ohnishi, H. J. F. Jansen, and A. J. Freeman, Phys. Rev. B **31**, 1168 (1985).

[14]H. Krakauer, Phys. Rev. B **30**, 6834 (1984).

[15]G. Treglia, M. C. Desjonqueres, and D. Spanjaard, J. Phys. C **16**, 2407 (1983).

[16]C. L. Fu, A. J. Freeman, E. Wimmer, and M. Weinert, Phys. Rev. Lett. **54**, 2261 (1985).

[17]A. Fasolino, G. Santoro, and E. Tosatti, Surf. Sci. **125**, 317 (1983).

[18]E. Tosatti, in *Karpacz Winter School of Theoretical Physics,* edited by A. Pekalski and J. Prizstawa (Springer, Berlin, 1979).

[19]L. D. Roelofs and S. C. Ying, Surf. Sci. **147**, 203 (1984).

[20]S. T. Ceyer, A. J. Melmed, J. J. Carrol, and W. R. Graham, Surf. Sci. **144**, L444 (1984).

[21]A. J. Melmed, S. T. Ceyer, R. T. Tung, and W. R. Graham, Surf. Sci. **111**, L701 (1981).

[22]P. Bak, Solid State Commun. **32**, 581 (1979).

[23]S. C. Ying and L. D. Roelofs, Surf. Sci. **125**, 218 (1983).

[24]L. D. Roelofs, G. Y. Hu, and S. C. Ying, Phys. Rev. B **28**, 6369 (1983).

[25]K. H. Lau and S. C. Ying, Phys. Rev. Lett. **44**, 1222 (1980).

[26]T. Inaoka and A. Yoshimori, Surf. Sci. **115**, 301 (1982); **149**, 241 (1985); T. Inaoka, M. Sawada, and A. Yoshimori, in *Dynamical Processes and Ordering on Solid Surfaces,* edited by A. Yoshimori and M. Tsukada (Springer, Berlin, 1985), p. 188.

[27]A. Fasolino, G. Santoro, and E. Tosatti, Phys. Rev. Lett. **44**, 1684 (1980).

[28]A. Fasolino, G. Santoro, and E. Tosatti, J. Phys. (Paris) Colloq. **6**, 846 (1981).

[29]S. Pick and M. Tomasek, Surf. Sci. **130**, L307 (1983); Czech. J. Phys. B **34**, 1235 (1984); **35**, 183 (1985).

[30]G. Y. Hu and S. C. Ying, Surf. Sci. **150**, 47 (1985).

[31]A. Fasolino and E. Tosatti, Surf. Sci. **178**, 483 (1986).

[32]N. D. Lang and W. Kohn, Phys. Rev. B **21**, 4555 (1970).

[33]E. Tosatti and P. W. Anderson, Solid State Commun. **14**, 773 (1974); see, e.g., E. Tosatti, in *Festkörperprobleme,* edited by O. Madelung (Pergamon, New York, 1975), Vol. 15, p. 113; in *Physics of Semiconductors,* edited by F. G. Fumi (North-Holland, Amsterdam, 1976), p. 21.

[34]W. A. Harrison, *Electronic Structure and the Properties of Solids* (Freeman, San Francisco, 1980), Chap. 20.

[35]J. Friedel, in *Theory of Magnetism in Transition Metals,* edited by W. Marshall (Academic, New York, 1967).

[36]C. M. Bertoni, C. Calandra, and F. Manghi, Solid State Commun. **23**, 255 (1977).

[37]It is interesting to note that also the fcc noble metals exhibit surface reconstruction, and one might be tempted to draw a connection. However, no covalent pseudogap exists in that case, and electron rehybridization at the surface is perfectly possible. In fact the reconstruction of Au, Ir, and Pt [see M. A. Van Hove, R. J. Koestner, P. C. Stair, J. P. Biberian, L. L. Kesmodel, I. Bartos, and G. A. Somorjai, Surf. Sci. **103**, 189 (1981)] appear not to be displacive in character, but rather to consist of a massive atom rearrangement which occurs to yield a better local packing.

[38]In general, a metal is not properly described by a two-body potential. However, it has been shown by Castiel *et al.* (Ref. 39) that, in fact, the bulk phonon properties for the particular case of W can be reproduced fairly well with a simple central two-body potential.

[39]D. Castiel, L. Dobrzynski, and D. Spanjaard, Surf. Sci. **59**,

252 (1976).

[40]*Handbook of Chemistry and Physics,* 66th ed., (CRC Press, Boca Raton, 1985), p. E-392; M. Lowrie and M. Gonas, J. Appl. Phys. **38**, 11 (1967).

[41]Equation (2) is clearly adequate only for small (R_i/R_i^0-1). The decrease of expansion beyond 1500 K is simply an artifact due to the lack of further terms in the expansion. This inaccuracy is irrelevant in the range of temperature and distortions of interest for surface reconstructions.

[42]C. Z. Wang, M. Parrinello, E. Tosatti, and A. Fasolino (unpublished).

[43]R. E. Allen and F. W. de Wette, Phys. Rev. **179**, 873 (1969).

[44]A. Fasolino, G. Santoro, and E. Tosatti, J. Phys. C **16**, 985 (1983).

[45]K. Binder and D. P. Landau, Surf. Sci. **151**, 409 (1985).

[46]This corrects an obviously incorrect statement made in Ref. 27.

[47]We note incidentally that the stability analysis should, strictly speaking, have been done for the relaxed surface, while the numerical results of Fig. 3, which reproduce our earlier calculations (Ref. 27), refer to the unrelaxed surface. However, the difference due to relaxation is negligibly small, as we have checked numerically.

[48]J. A. Walker, M. K. Debe, and D. A. King, Surf. Sci. **104**, 405 (1981).

[49]This point is actually somewhat controversial. See Ref. 28 but also R. T. Tung, W. R. Graham, and A. J. Melmed, Surf. Sci. **115**, 576 (1982); P. J. Estrup, L. D. Roelofs, and S. C. Ying, Surf. Sci. **123**, L703 (1982); A. J. Melmed and W. R. Graham, *ibid.* **123**, L706 (1982).

[50]K. Griffiths, D. A. King, and G. Thomas, Vacuum **31**, 671 (1981).

[51]J. J. Arracis, Y. J. Chabal, and S. B. Christman, Phys. Rev. B **33**, 7906 (1986).

[52]J. F. Wendelken and G. C. Wang, J. Vac. Sci. Technol. A **2**, 886 (1984).

[53]P. C. Stephenson and D. W. Bullett, Surf. Sci. **139**, 1 (1984).

[54]B. Legrand, G. Treglia, M. C. Desjonquieres, and D. Spanjaard (unpublished).

[55]See, e.g., R. A. Cowley, Adv. Phys. **29**, 1 (1980).

[56]J. V. José, L. P. Kadanoff, S. Kirkpatrick, and D. R. Nelson, Phys. Rev. B **16**, 1217 (1977).

[57]S. Krinsky and D. Mukamel, Phys. Rev. B **13**, 5065 (1976).

[58]O. Hudak, J. Phys. C **16**, 2641 (1983); **16**, 2659 (1983).

[59]S. Aubry, F. Axel, and F. Vallet, J. Phys. C **18**, 753 (1985).

[60]P. Bak, Rep. Prog. Phys. **45**, 587 (1982).

[61]S. C. Ying, in *Dynamical Phenomena at Surfaces, Interfaces and Superlattices,* edited by F. Nizzoli, K. H. Rieder, and R. F. Willis (Springer, Berlin, 1985), p. 148.

[62]P. J. Estrup, J. Vac. Sci. Technol. **16**, 635 (1979).

[63]We thank S. Doniach (private communication) for pointing this out to us.

[64]See, e.g., V. Heine, in *Group Theory in Quantum Mechanics,* (Pergamon, Oxford, 1964), Chap. VI-26.

[65]J. P. Woods and J. L. Erskine, Phys. Rev. Lett. **55**, 2595 (1985); J. Vac. Sci. Technol. A **4**, 1414 (1986).

[66]V. Heine, and J. C. D. McConnell, Phys. Rev. Lett. **46**, 1092 (1981); V. Heine and J. D. C. McConnell, J. Phys. C **17**, 1199 (1984); V. Heine, R. M. Lynden-Bell, J. D. C. McConnell, and I. R. McDonald, Z. Phys. B **56**, 229 (1986).

[67]B. N. Brockhouse, in *Phonons in Perfect Lattices and Lattices With Point Imperfections,* edited by R. W. H. Stevenson (Oliver&Boyd, Edinburgh, 1966), p. 110.

[68]G. F. Koster, J. O. Dimmock, R. G. Wheeler, and H. Statz, *Properties of the Thirty-two Point Groups* (M.I.T. Press, Cambridge, Mass., 1963).